Structure and mechanics of interfaces in biological materials

Francois Barthelat[1], Zhen Yin[1] and Markus J. Buehler[2]

Abstract | Hard biological materials — for example, seashells, bone or wood — fulfil critical structural functions and display unique and attractive combinations of stiffness, strength and toughness, owing to their intricate architectures, which are organized over several length scales. The size, shape and arrangement of the 'building blocks' of which these materials are made are essential for defining their properties and their exceptional performance, but there is growing evidence that their deformation and toughness are also largely governed by the interfaces that join these building blocks. These interfaces channel nonlinear deformations and deflect cracks into configurations in which propagation is more difficult. In this Review, we discuss comparatively the composition, structure and mechanics of a set of representative biological interfaces in nacre, bone and wood, and show that these interfaces possess unusual mechanical characteristics, which can encourage the development of advanced bioinspired composites. Finally, we highlight recent examples of synthetic materials inspired from the mechanics and architecture of natural interfaces.

Biological materials display highly controlled structural features over several length scales, including down to the nano- and molecular scales. These materials show advanced properties despite being composed of modest ingredients and boast performances that are in some ways superior to those of engineering materials[1–7]. In addition, biological materials can adapt their composition and structure to their environment, and can self-repair and remodel. In terms of absolute structural performance, hard biological materials, such as bone or mollusc shells, are in general inferior to engineering materials, for example, steels or fibre-reinforced composites. However, the mechanical performance of hard biological materials is much higher than that of their components — brittle minerals and weak proteins — and it is this 'property amplification' achieved by these natural composites that is remarkable. In particular, biological materials are strong and tough — two properties that are typically mutually exclusive in engineering materials[8] (BOX 1). The structure and mechanics of biological materials have traditionally been characterized in terms of building blocks of finite size that are ordered into well-controlled arrangements, much like individual bricks in a wall. Nature tightly controls the size, shape and arrangement of these blocks and, as a result, the term 'architecture' is increasingly used instead of the term 'microstructure', which is traditionally used in materials science[9,10]. This concept has been introduced as the universality–diversity paradigm[11]; according to this, a vast diversity of properties is achieved by arranging a limited set of 'universal' structural motifs at distinct length scales, often concurrently at multiple scales. In proteinaceous materials, these structural motifs include helices, crystals or disordered regions. At larger length scales, structural motifs have recently been classified into fibrous, helical, gradient, layered, tubular, cellular, suture and overlapping[9] building blocks. Owing to the combination of these structural motifs over multiple scales, natural materials achieve high performance at the macroscale[9,12,13].

In addition to these sophisticated architectures, it has now become evident that the deformation and fracture of these materials are largely governed by the interfaces contained within them[10,14–16]. These interfaces may occupy a very small volume fraction in the material, but their importance is such that in recent work interfaces are themselves described as their own building block[17]. For example, proteins in enamel comprise just 1% of total enamel weight, and proteins taken from the interface between crystallite and rods have been shown to be critical for the overall toughness of the enamel, as removing these proteins results in a 40% decrease in fracture toughness[18]. Nacre from mollusc shells is another example of a hard but extremely tough material[19,20]. It is mostly made of microscopic tablets of calcium carbonate, and organic materials — which constitute only 5% of the total volume — serve as 'mortar' between the tablets[21]. The deformability of the thin organic mortar is crucial for overall

[1]*Laboratory for Advanced Materials and Bioinspiration, Department of Mechanical Engineering, McGill University, 817 Sherbrooke Street West, Montreal, Quebec H3A 2K6, Canada.*
[2]*Laboratory for Atomistic and Molecular Mechanics, Department of Civil and Environmental Engineering, 77 Massachusetts Avenue, Massachusetts Institute of Technology, Cambridge, Massachusetts 02139, USA.*
Correspondence to F.B.
francois.barthelat@mcgill.ca

Article number: 16007
doi:10.1038/natrevmats.2016.7
Published online 8 Mar 2016

© 2016 Macmillan Publishers Limited. All rights reserved

performance, and dehydrating the organic interfaces turns nacre from a quasi-ductile composite into a very brittle material similar to pure calcium carbonate[22]. Hard biological materials are packed with organic-rich interfaces that can glide and slide. These interfaces operate in synergy with specific architectures in the materials, providing nonlinear deformation mechanisms and turning inherently brittle materials into materials that can deform inelastically, redistribute stresses around defects and dissipate energy. Interfaces can also deflect cracks and channel them into configurations in which their propagation is hindered or arrested, generating tougher materials. In a material such as bone, these principles can be observed simultaneously over several hierarchical length scales[15,23,24]. Recent material models seek to incorporate the mechanical behaviour of biological interfaces explicitly[17,25], and the development of bioinspired materials is increasingly focused on duplicating the features, mechanisms and properties of natural interfaces[26–30]. However, the composition, structure, properties and mechanics of biological interfaces are often complex and difficult to investigate, mainly because of their small thicknesses. There are still gaps in our quantitative understanding of the role of these interfaces, and there are associated controversies in our understanding of how they are constructed and how they operate.

Here, we review the composition, structure, mechanics and properties of three representative examples of biological interfaces: nacre, bone and wood. We then discuss some general characteristics of these interfaces, which can serve as guidelines for the design of bioinspired composites.

The interfaces in nacre

Mollusc shells are mostly made of minerals (at least 95% by volume) and contain only a small fraction of organic materials (at most 5% by volume)[31]. Among the materials found in mollusc shells, nacre is the strongest and toughest[31] (FIG. 1). Nacre displays complex micromechanisms of deformation and fracture that generate high stiffness (70–80 GPa), high tensile strength (70–100 MPa) and high fracture toughness (4–10 MPa $m^{1/2}$)[19,21,32]. However, nacre has a relatively simple brick-wall-like architecture composed of mineral polygonal tablets (0.2–1 μm in thickness and 5–10 μm in diameter; see FIG. 1a,b). The tablets are not perfectly flat and display a considerable waviness that can reach 200 nm in amplitude[22]. For many years, these tablets were thought to be made of large crystals of aragonite[1]; however, the tablets are actually 'mesocrystals' composed of nanograins with the same crystallographic orientation, thereby featuring another level of hierarchical structuring (FIG. 1e). The nanograins are delimited by organic materials[33,34] that constitute the intracrystalline fraction of the total organic content in the material[35]. Forming the bulk of the tablets, the nanograins emerge at the surface of the tablets as nanoasperities[19]. Under tension, the tablets can slide on one another, which generates relatively large deformations

Box 1 | **Stiffness, strength and fracture toughness**

The basic mechanical properties of structural materials are stiffness, strength and fracture toughness. Stiffness characterizes the resistance to elastic deformations; strength characterizes the onset of stress required to permanently deform the material (either by inelastic deformation or by fracture); and fracture toughness is the ability of the material to resist the propagation of cracks. In general, stiffness and strength are governed by the strength of interatomic interactions in the material, and therefore the stiffest materials also tend to be the strongest[169]. Fracture toughness is a property that is sometimes confused with strength — it is defined as the energy required to propagate a crack within a material. Strength and toughness are properties that are usually mutually exclusive[8], because strong materials typically fracture before they can deform significantly. Materials with low strength enable inelastic deformations, which can redistribute stresses around stress concentrators, defects and cracks, making their propagation more difficult and therefore increasing fracture toughness. Ductile materials show strong resistance to cracking and can deform inelastically to large strains, which confers damage tolerance, reliability and resistance to impacts. For example, steel is a material that balances strength and toughness. There are several methods to strengthen steel (that is, increase yield stress), but they are all accompanied by a decrease in toughness. High-strength steels are very brittle and sensitive to defects, making them a poor design choice for most applications. Likewise, diamond is one of the stiffest and strongest substances known, but it is also brittle.

There has been an intense research effort for methods that can achieve new combinations of stiffness, strength and toughness. The resulting materials are inhomogeneous, with several distinct phases (for example, carbon fibres in an epoxy matrix) or weak interfaces (such as layered ceramics). Incorporating weak interfaces within materials is a powerful approach used to deflect cracks and control toughening mechanisms. For example, weak grain boundaries in aluminium oxide increase overall toughness[170], controlled debonding of the interface fibre matrix generates crack bridging and pullout[170], and planar interfaces in ceramics can deflect incoming cracks and increase toughness by orders of magnitude[171]. The properties of these materials result from a trade-off between strength and toughness. Strong interfaces are required to ensure adequate load transfer and strong cohesion for the material, but the interfaces must also be weak enough to debond ahead of propagating cracks[172], to deflect cracks[151] and to enable inelastic shear deformations between the fibres and the matrix[170]. For example, in fibre-reinforced materials, the interface between the fibres and the matrix must be strong enough to ensure stress transfer to the fibres and overall strength, but weak enough to enable inelastic deformation that can redistribute stresses around holes, notches, defects and cracks[155]. Strong interfaces lead to brittleness[173], and 'pseudo-ductile' composites are preferred for their robust design and damage tolerance[155,174]. Although the weak interfaces in synthetic materials are generally brittle and have relatively simple geometries, in natural materials the architecture of the interfaces is more sophisticated, and the inclusion of organic materials confers inelastic deformation capabilities.

© 2016 Macmillan Publishers Limited. All rights reserved

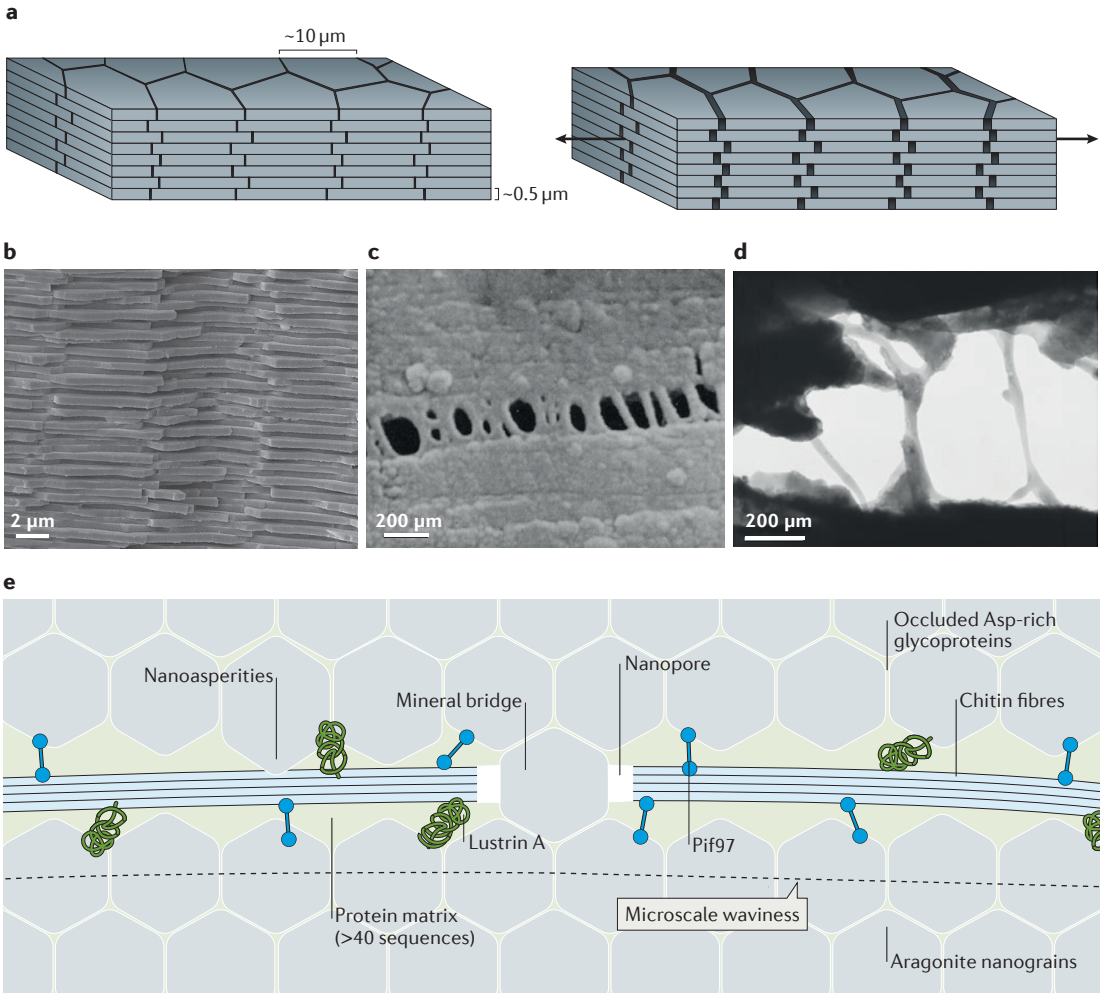

Figure 1 | **The structure, deformation and interfaces of nacre. a** | A schematic of the brick-and-mortar structure of nacre. The deformation of nacre under tension is dominated by the sliding of the mineral tablets on one another. **b** | A scanning electron microscopy (SEM) image of the fracture surface of red abalone nacre[22]. **c** | Separating the tablets in the out-of-plane direction reveals a highly deformable matrix. The SEM image shows the formation of cavities and ligaments[32]. **d** | The ligaments can elongate to great lengths. In this transmission electron microscopy image, the ligaments are up to 500 nm long, which is more than 10 times the initial thickness of the interface[49]. **e** | A schematic of the interfaces in nacre. Panel **b** is reproduced with permission from REF. 22, Elsevier. Panel **c** is from REF. 32, Jackson, A. P., Vincent, J. F. V. & Turner, R. M., The mechanical design of nacre, *Proc. R. Soc. Lond. B*, 1988, **234**, by permission of the Royal Society. Panel **d** is from REF. 49, Nature Publishing Group.

(up to almost 1% strain) accompanied by energy dissipation[19,22,32]. Other deformation mechanisms associated with the nanostructure of the tablets have been proposed[36]; however, if these were to occur under tension, their contribution to the overall tensile deformation would be much smaller than that of tablet sliding.

The relatively simple mechanism of tablet sliding leads to crack bridging and process-zone toughening[37], two powerful toughening mechanisms that make nacre several orders of magnitude tougher than aragonite[19,20,38]. The sliding and pullout of the tablets are mediated by the thin (20–40 nm) interfaces between the tablets, which are rich in organic materials[39]. These organic materials are highly deformable and strongly adhere to the tablets, as shown by the formation of long ligaments when the interface is opened (mode I fracture) (FIG. 1c,d). Complete cleavage of the interface exposes organic materials on both fractured surfaces[16,40], which also confirms that these materials strongly adhere to the surface of the tablets. The toughness of the interfaces[2,16,21] in mode I fracture is about 10 J m^{-1}, which is roughly two orders of magnitude less than the toughness of nacre[38]. Weak interfaces are a requirement for the ability to deflect and guide incoming cracks (BOX 1). Under shear, the interfaces deform elastically up to a yield point of about 10–20 MPa, followed by a region of large strains accompanied by strain hardening up to a maximum shear stress of 30–50 MPa (REFS 19,22,41). Mechanical tests on demineralized nacre confirm that the organic materials have low strength but high deformability[16,42]. However, in demineralized nacre, the organic material is not confined, and its mechanical response may not fully reflect

© 2016 Macmillan Publishers Limited. All rights reserved

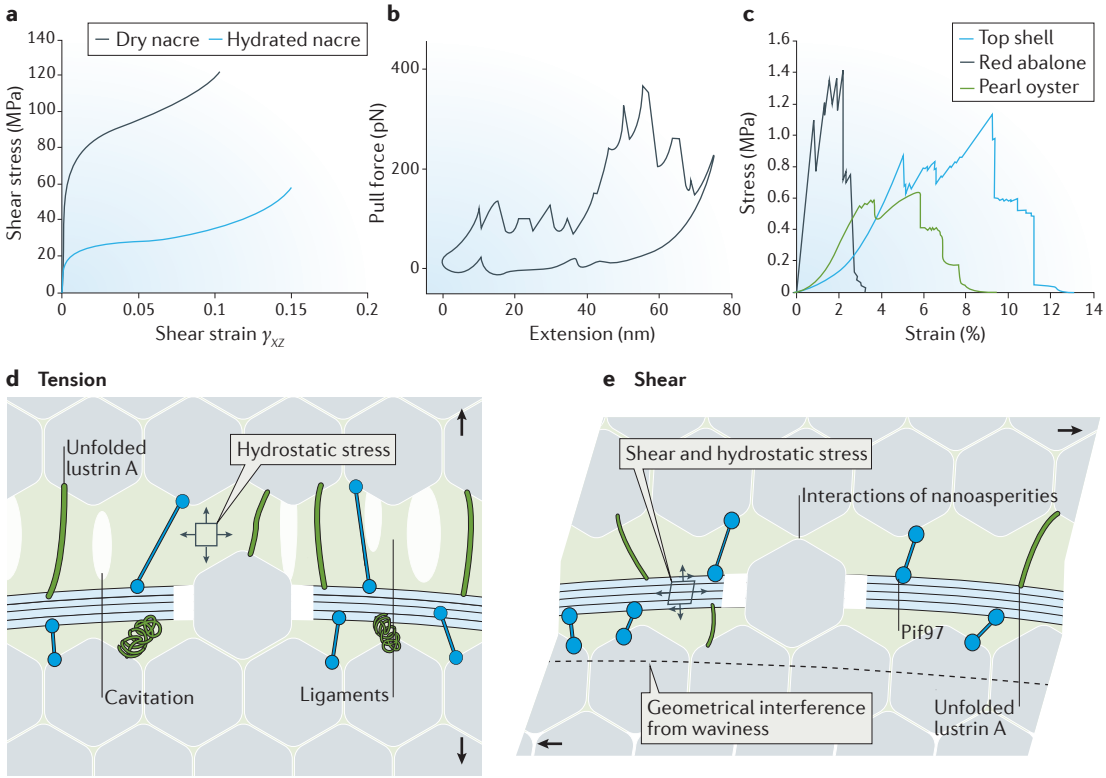

Figure 2 | **Mechanical tests on the interfaces in nacre. a** | Deforming nacre under shear along the interfaces reveals large strains and strain hardening[22]. **b** | A microcantilever in an atomic force microscope is used to pull individual molecules from cleaved nacre surfaces. The force–extension curves reveal a saw-tooth pattern characteristic of the breakage of sacrificial bonds[49]. **c** | Tensile tests on demineralized nacre showing low strength but large extensions[16]. **d** | Possible deformation mechanism for the interfaces in nacre when subjected to tension. **e** | Possible deformation mechanism for the interfaces in nacre when subjected to shear. Panel **a** is adapted with permission from REF. 22, Elsevier. Panel **b** is from REF. 49, Nature Publishing Group. Panel **c** is adapted with permission from REF. 16, Elsevier.

the mechanical response of the same material under nanoconfinement from the tablets[43]. The low strength of the interfaces is crucial to ensure that deformation and cracking occur at the interface[44], and high extensibility is essential to develop inelastic mechanisms over large volumes and to generate toughness at the macroscale[22]. Among other properties of the interfaces in nacre, it has been suggested that extensibility is the most important for the overall toughness of nacre[45]. The properties of the interfaces seem to be fine-tuned to achieve a high-performance material[45], much like the interfaces between fibres and the matrix in engineering composites must be optimized (BOX 1). Disrupting this balance by desiccating the organic layers results in a stronger but more brittle material[22]. By contrast, removal of the organic materials — for example, by thermal treatment — leads to a sharp drop in strength and modulus[46].

The accepted model for the organic interfaces between layers of tablets consists of a layer of β-chitin fibrils sandwiched between two proteinaceous layers (FIG. 1e). The proteinaceous layers are bonded to the tablets, forming a continuous connection with the intracrystalline network[1,34,35,39]. About 40 protein sequences have been identified so far, and further sequences remain to be identified[47]. The mechanical response of the interface can be assessed by shear tests on samples of nacre[22] (FIG. 2a). The response is strongly dependent on hydration, which suggests that the organic layer carries a significant portion of the shear stress. Under shear, the interfaces display a yield point (of about 20 MPa under hydrated conditions and 60 MPa under dry conditions), followed by hardening and failure at relatively large strains (10%). The two organic components that are most cited in relation to the mechanical properties of the interfaces in nacre are chitin[39] and lustrin A[48,49]. Chitin is a polysaccharide that is very stiff and strong under tension and is the main component in arthropod cuticles[50]. In nacre, chitin is in the form of a dense mat of nanofibres interspersed with nanopores[51]. Chitin is believed to serve as reinforcement for the organic template before biomineralization[52], but its function in fully grown nacre is less clear. Molecular pull tests on the interfacial organic molecules, which are exposed by cleaving nacre, have revealed large extensibility and 'saw-tooth' patterns in the force–extension curve, which are characteristics of molecules with sacrificial bonds and 'hidden length', such as lustrin A[49] (FIG. 2b). The unfolding of lustrin A is only initiated at a critical tensile force, which translates into a macroscale yield point for the proteinaceous mixture[53]. The large deformation generated by the sequential unfolding of lustrin A is believed to underlie the formation of ligaments in the organic

© 2016 Macmillan Publishers Limited. All rights reserved

materials[49] and may explain its high extensibility under tension (FIG. 2c), although the large strains observed under tension may also be a result of substantial deformations of the nanopores[54]. Proteins, polysaccharides and the mineral are tightly bonded at the interfaces. The adhesion of the proteinaceous layers to the mineral is strong, partly because they form a continuous network with the intracrystalline proteins. The proteinaceous layers are also tightly bonded to the chitin layer, possibly through covalent bonds[55]. In addition, another key protein called Pif97, which has both chitin-binding sites[56] and aragonite-binding sites[57], may function as a crosslinker between chitin and aragonite[28,58]. Under tension, cavities rapidly grow in size[54] and turn into ligaments, providing cohesion over large deformations (FIG. 2d). This behaviour is consistent with an elastomeric adhesive confined between two adherents and stretched under tension (BOX 2), with strong adhesion to the surface of the tablets. Chitin is relatively stiff and brittle, and thus the formation of ligaments probably takes place within the proteinaceous layers.

Interestingly, although synthetic elastomers produce a linear response under shear even at large deformations (BOX 2), the shear response of biological elastomers containing sacrificial bonds exhibits a yield point and extremely large shear deformations[53]. A possible function of chitin could be to delay the shear fractures that can occur from the tensile stress that builds up as the interface is sheared[59,60]. At the microscale, the resistance to sliding is generated, in part, by the waviness of the tablets, which produces progressive interlocking[22]. At other regions and mostly at the centre of the tablets, nanobridges of aragonite connect adjacent tablets[51,61]. The interfaces in nacre are complex nanoscale subsystems composed of a network of proteins and polysaccharides with functions in both the growth and the mechanical strength of the material.

The interfaces in bone

Bone is a high-performance material that has various functions, the primary of which is mechanical support[62]. To fulfil this supporting role, bone is stiff and hard because of its mineral content, but it is also surprisingly tough[63] considering its content of brittle minerals and soft proteins. By weight, approximately 60% of bone is composed of mineral (calcium and phosphate), 10–20% of water and 20–30% of proteins. About 90% of the protein content is type I collagen, and the remaining 10% is non-collagenous proteins, including fibronectin, osteonectin, sialoprotein, osteocalcin and osteopontin[64]. Bone density and mineral content have long been used as the only predictors of bone strength; however, these measures have limitations (not discussed here)[65]. More recent research has considered bone as a composite material in which minerals, collagen and extracollagenous proteins contribute to its mechanical performance[15,66]. Bone has a complex hierarchical structure[23,24] (FIG. 3) with 3D features that are yet to be fully elucidated[67]. At the molecular scale, individual collagen molecules (known as tropocollagen) interact through coordinated hydrogen bonds[68] and self-assemble into fibrils (FIG. 3). Specific covalent crosslinks at the ends of the collagen molecules (telopeptide regions) provide cohesion and mechanical stability to the fibrils, and govern complex unravelling nanomechanisms as the fibrils are stretched[69]. Collagen fibrils are relatively stiff and strong[70], and they are further reinforced by nanocrystals of hydroxyapatite[23,71,72] following mineralization processes that are controlled by the arrangement of the collagen molecules as well as their crosslinking[73]. The fibrils bundle into fibres, which form the building blocks of bone at the next hierarchical level. In turn, the fibres arrange into cross plies and lamellae at the microscopic scale (FIG. 3). Lamellae wrap around the Haversian canals concentrically to form the osteons, which are the microscopic building blocks of mature

Box 2 | **The mechanics of adhesive bonds**

Modern adhesives are now used increasingly to assemble structural components. Compared with other joining methods, adhesively bonded joints are light, they generate little stress concentrations, and they are more resistant to fatigue[175]. Engineering adhesives include a large number of formulations: for example, thermoplastics, thermosetting resins and elastomeric compounds. In engineering, the deformation, and thus the failure, of adhesive bonds depends on the mechanical properties of the polymer used as an adhesive, the type and strength of the bond on the adherent (such as micro-interlocking and chemical bonds), and the loading condition (for example, stress state, loading rate, temperature or moisture). A bonded joint may fail because of adhesive failure (the adhesive detaches from the adherent), cohesive fracture (fracture runs within the adhesive layer) or adherent failure (fracture runs within the adherent substrate). Soft elastomeric or ductile engineering adhesives are those that are the closest, in terms of behaviour, to the organic interfaces encountered in natural materials. For this class of adhesives, cohesive failure is more desirable than adhesive failure because cohesive failure benefits from the properties of the adhesive (such as enabling large deformation, energy absorption capabilities and damping). The yielding of ductile adhesives is governed by maximum shear stress and also by hydrostatic stresses: in the presence of tensile stresses, the material may fail by the formation of crazes, making the material weaker in tension than in shear. Ductile bond lines can accommodate stress concentrations at, for example, the ends of a lap joint. Another major class of adhesives is elastomers. Although the deformation of elastomeric bonds can be large, their deformation is recoverable and governed by entropic elasticity. Elastomers are close to incompressible; therefore, the only way to accommodate separation of the adherent under confined conditions is by the formation of cavities[176], which can elongate and form ligaments across the interfaces. The formation of ligaments prevails over adhesive failure in adhesives with low modulus — that is, with lower molecular weight and/or reduced crosslinking[175]. Under simple shear, elastomers exhibit a linear stress–strain curve even at large strains[59,177], as well as hydrostatic tension[59], which can cause failure by cavitation. Such failure was recently observed experimentally on lap joints, in the form of tilted cracks[60] and at the elastomeric interfaces of nacre-like 3D printed materials[7,163,178–180].

© 2016 Macmillan Publishers Limited. All rights reserved

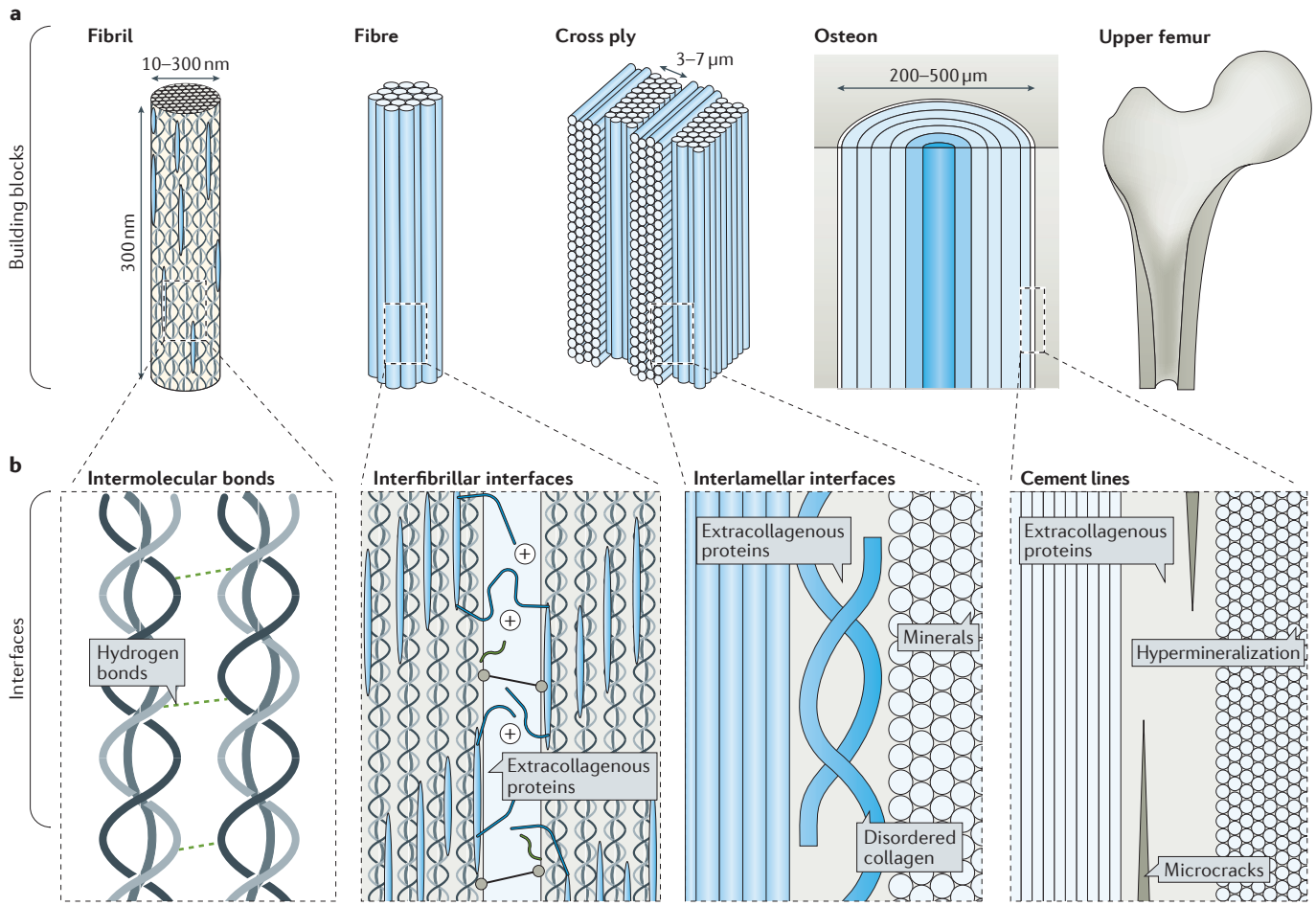

Figure 3 | **The building blocks and interfaces of bone. a** | Bone has a hierarchical structure with building blocks that range from nanometres to hundreds of micrometres in size: fibril, fibre, cross ply and osteon. **b** | The interfaces within each of these hierarchical structures, at different length scales, are shown. These interfaces differ in composition and size, but their function is the same: to transfer mechanical stresses between building blocks and across length scales. Panel **b** is adapted with permission from REF. 24, Elsevier.

cortical bone. Small-scale and *in situ* experiments, micromechanics and fracture mechanics have successfully captured the structural features governing the deformation and fracture of bone over these multiple length scales[15,74–76]. Notably, the results of these experiments highlight the importance of the interfaces between these building blocks, which may be at least as crucial as the building blocks themselves for overall mechanical performance[14,72,77–81]. Here, we focus on the composition, structure and mechanics of two of the critical interfaces within bone: the interfibrillar interfaces and the cement lines.

Interfibrillar interfaces. Collagen fibres comprise bundles of fibrils that are held together by a 1–2 nm thick layer of non-collagenous interfibrillar matrix (FIG. 3). This proteinaceous adhesive is amorphous and contains various proteins, including osteocalcin and osteopontin[75]. This mixture of proteins is more compliant and weaker than the stiff, mineralized and aligned collagen fibrils, as demonstrated by the cleavage and fracture surfaces of lamellar bone at the microscale[81]. The proteins at the interfaces are, however, highly deformable, and separating the collagen fibrils in bone forms ligaments in the interfaces[81] (FIG. 4a); these observations are similar to those for nacre (FIG. 1c,d). *In situ* X-ray tensile testing on femoral bovine bone demonstrated that the shearing of the interfibrillar interfaces accounts for up to 60% of the overall tensile deformation of bone[82], a 'nanoscale ductility' that is key to energy dissipation and to the formation of dilation bands at the nanoscale[83,84]. Propagating a crack in bone involves the pullout of individual fibres and fibrils from the crack faces[85,86] as well as bridging, which increase the overall toughness of bone.

The pullout process is similar to the fracture processes in fibre-reinforced composites, which require the presence of weak interfaces between fibres and the matrix (BOX 1). It is difficult to obtain direct measurements of the mechanical properties of the interfibrillar interfaces. Pullout tests on individual collagen fibrils from antler bone reveal a shear strength of about 0.65 MPa (REF. 87), which is much less than the macroscopic strength of antler bone (200–300 MPa)[63]. The composition and the structure of the interfibrillar interfaces remain to be fully elucidated, but osteocalcin and osteopontin seem to be

© 2016 Macmillan Publishers Limited. All rights reserved

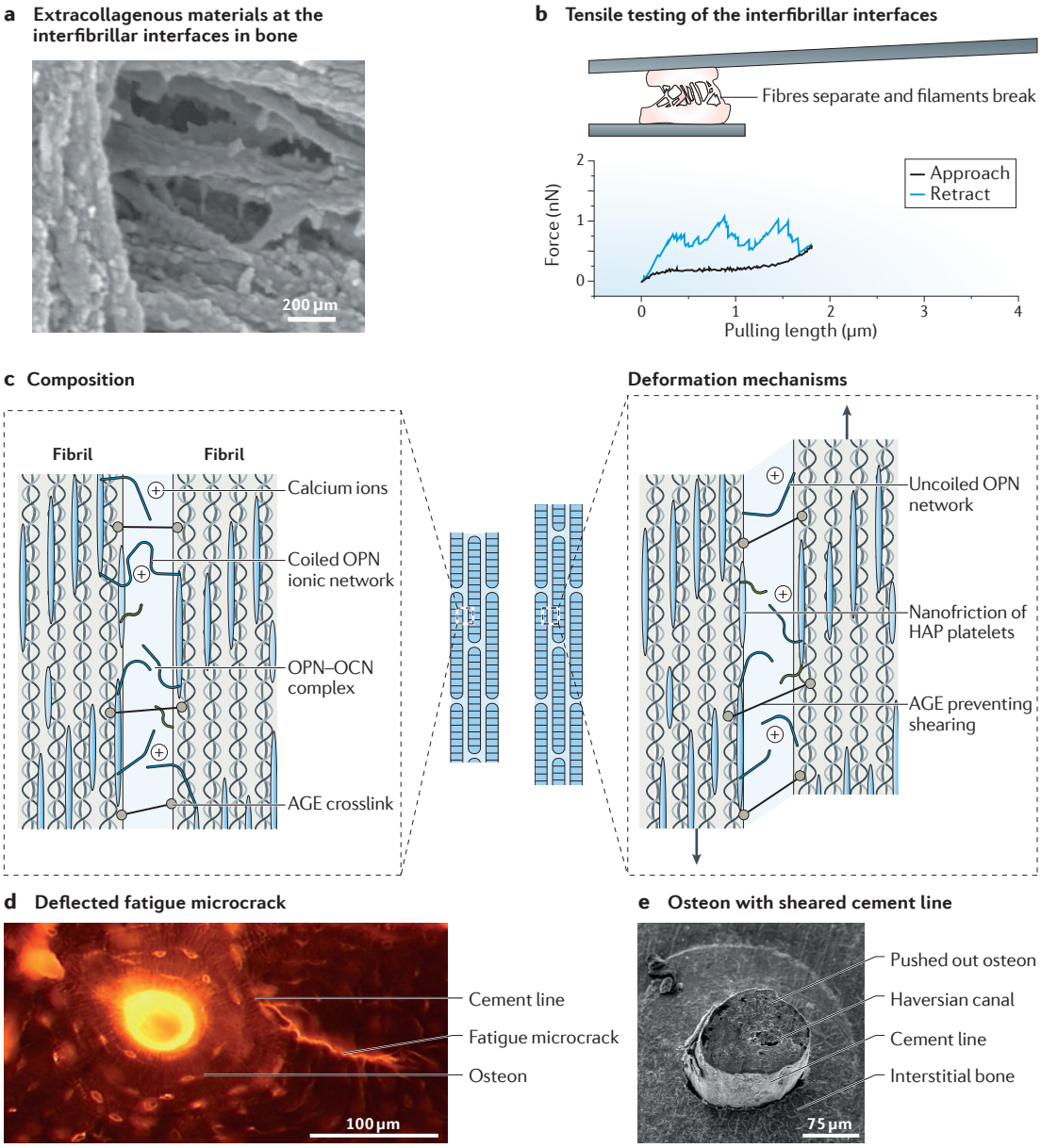

Figure 4 | **The mechanics of the interfaces within bone. a** | Separating the collagen fibrils exposes highly deformable materials at the interfibrillar interfaces[81]. **b** | Tensile testing on this interface reveals large extensions and the saw-tooth pattern characteristic of the breaking of sacrificial bonds, which can re-form upon unloading[81]. **c** | A schematic of the interfibrillar interface showing some of its main structural components (left panel). The main deformation mechanisms at the interfibrillar interface under shear are shown in the right panel. **d** | A fatigue microcrack is deflected into a cement line[109]. Cement lines are preferred sites for microcracks. **e** | An out-of-position individual osteon after a push-out test in which the cement line is sheared[107]. AGE, advanced glycation end product; HAP, hydroxyapatite; OCN, osteocalcin; OPN, osteopontin. Panels **a** and **b** are from REF. 81, Nature Publishing Group. Panel **d** is reproduced with permission from REF. 109, Elsevier. Panel **e** is reproduced with permission from REF. 107, Elsevier.

key to the mechanics of these interfaces. Osteocalcin and osteopontin can form a complex that promotes the adhesion of the mineral to collagen[88]. Osteopontin strongly adheres to hydroxyapatite, and it is decorated with negative charges that can form sacrificial bonds with positively charged calcium ions[89]. If the interface is opened or shear is applied, these electrostatic sacrificial bonds can break and release hidden lengths along the molecule, generating the saw-tooth pattern observed experimentally[81] (FIG. 4b). Tensile experiments on bovine cortical bone using stepwise changes in strain rates confirmed that the activation enthalpy associated with nonlinear deformation in bone corresponds to the disruption of electrostatic bonds[90]. Interestingly, these bonds can re-form rapidly[81], effectively healing bone at the nanoscale without the need for remodelling[91,92]. Experiments have shown that suppressing the actions of these proteins has a considerable impact on the overall performance of bone, with

© 2016 Macmillan Publishers Limited. All rights reserved

a significant decrease in deformability and energy dissipation capabilities at the molecular scale[81,93], a decrease in diffuse damage at the sub-micrometre scale[83] and a decrease in toughness at the macroscale[94].

Other mechanisms may also contribute to the mechanics at the interfibrillar interfaces. More specifically, the collagen fibrils are largely covered by hydroxyapatite nanocrystals[71], and, as a result, it is conceivable that the sliding of the fibrils on one another involves direct contact between nanocrystals of adjacent fibrils, which would generate frictional resistance to sliding[95] in a similar way to nacre[19]. Finally, additional contributions to bonding slowly develop over time. Ageing collagen is subject to slow non-enzymatic glycation, which generates advanced glycation end products (AGEs), such as pentosidine. AGEs increase the degree of crosslinking between collagen molecules and between collagen fibrils[96]. This makes the interfibrillar interface stiffer and stronger but also hinders nanoscale deformations[78] and reduces diffuse microdamage[97]. As a result, ageing bone tends to be stiffer and stronger but more brittle[78,97]. The interfibrillar interfaces in bone are therefore complex systems in which several mechanisms concurrently contribute to tensile and shear responses (FIG. 4c).

Interfibrillar interfaces also govern the deformation and fracture of collagenous materials other than bone. For example, tendons are made of unidirectional collagen fibrils, and the interfaces between these fibrils are crucial for the deflection and blunting of incoming cracks, and to channel deformations[98,99]. In fish scales, the collagen fibrils form cross plies, and the interfaces between the fibrils govern defibrillation, pullout, delamination and rotation of adjacent laminates[100,101]. Tendons and fish scales are among the toughest biological materials known[98,100], and this toughness results from powerful toughening mechanisms that are principally governed by the interfaces between collagen fibrils.

Cement lines. Bone accumulates fatigue microcracks from the repeated mechanical loads associated with normal activities[79]. The negative effects of this damage on the performance of bone are compensated by remodelling, a process by which old bone material is replaced by new bone. Remodelling is performed by the bone remodelling units that consist of osteoclast cells and osteoblast cells. Osteoclast cells dissolve and digest 'old' bone, and osteoblast cells generate 'new' bone by depositing collagen fibrils, which mineralize after deposition. These bone remodelling units migrate along the direction of long bones, leaving cylindrical wakes of newly remodelled bone, the osteons. Osteons are lined with a 1–5 μm thick boundary called the cement line, which functions as an interface between the osteons and the surrounding interstitial bone[102,103]. Mature cortical bone can therefore be interpreted as a unidirectional fibre-reinforced composite (BOX 1), in which the osteons are the fibres and the interstitial bone is the matrix[104]. Similarly to the way that an interface composed of carbon or glass fibres in synthetic composites can deflect cracks and generate toughness by pullout, cracks can be deflected or twisted along the weaker cement lines[74,105] (FIG. 4d). These powerful mechanisms make cortical bone five times tougher in the transverse direction than in the longitudinal 'splitting' direction[76].

To deflect incoming cracks properly, the cement line must be considerably weaker than both the osteons and the interstitial bone. The shearing behaviour of the cement line can be evaluated by pushing the osteon along its axis and out of its interstitial bone surrounding using thin cross sections of cortical bone[106,107] (FIG. 4e). This test revealed that the shear strength of the cement lines (8 MPa) is an order of magnitude lower than that of the surrounding interlamellar interfaces within the osteon (73 MPa)[108]. Once the cement line has broken, frictional pullout ensues[107], a mechanism that is also observed and exploited in synthetic fibres used in engineering composites. The fracture toughness of cement lines can be estimated from the toughness of cortical bone in the splitting direction because, in that orientation, the crack mostly propagates along the cement lines. By this measure, the toughness of the cement line is 1–2 MPa $m^{1/2}$, which is an order of magnitude lower than the toughness of bone in the transverse direction[105]. These experiments confirm the strong contrast between the strength of cement lines and that of the surrounding bone material, which can be explained by differences in composition and structure. Cement lines are more mineralized than the surrounding bone[103], which makes them more brittle. Short microcracks are typically deflected by the cement line[109], where they accumulate preferentially[110,111]. They also have lower collagen content than their surroundings and a high level of non-collagenous proteins, including osteocalcin, osteopontin and bone sialoprotein[103]. The combination of lower collagen content, higher mineralization and the accumulation of damage explains why cement lines are so much weaker than the surrounding bone. The main toughening mechanisms associated with the cement line are crack deflection and twisting[15,105,112], although debonding followed by frictional pullout has also been suggested as an important toughening mechanism associated with osteons[113,114].

Bone has been historically interpreted as a ceramic, then as a composite of mineral and collagen, and then as a hierarchical structure with building blocks at distinct length scales. This hierarchy of structures and mechanisms gives rise to unusual combinations of high stiffness, high strength and high toughness[3,115,116]. Recent studies on the mechanics of bone[15,105] suggest a picture in which the interfaces between the building blocks operate synergistically to produce a high-performance material. The ductile deformation of bone is governed by nonlinear mechanisms at the nanoscale, with the interfibrillar interfaces as the main contributor[84]. By contrast, fracture appears to be governed by the brittle and fragile cement lines around the osteons, which deflect and twist incoming cracks[15,105,112]. Other mechanisms, such as crack deflection on the collagen lamellae within osteons[117], confined microcracking[118], pullout of collagen fibrils[85] and pullout of osteons[113,114], have also been suggested. However, experiments and fracture-mechanics models suggest that crack deflection and twisting are the primary toughening mechanisms for cortical bone[15,105,112].

© 2016 Macmillan Publishers Limited. All rights reserved

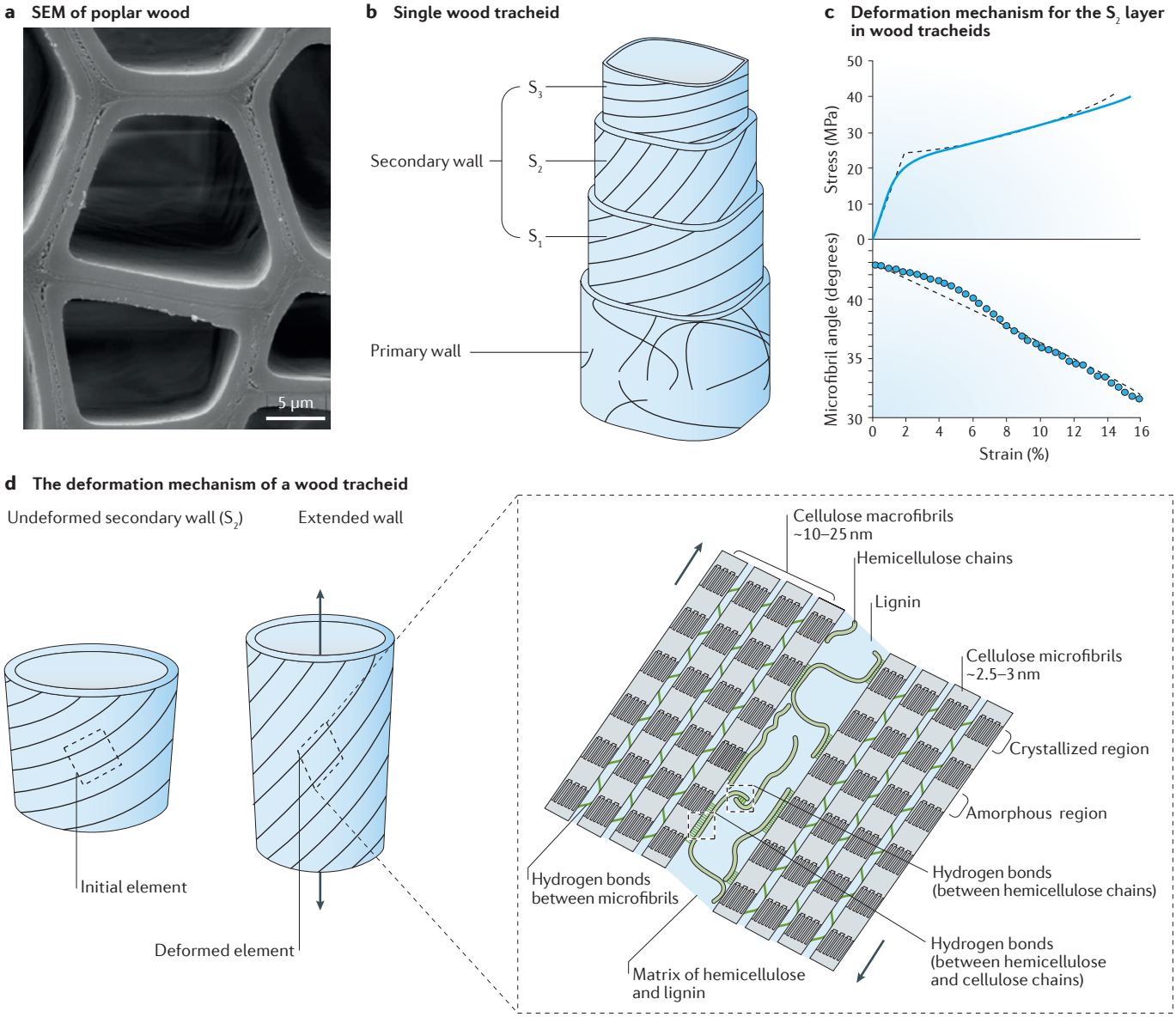

Figure 5 | **The structure and mechanics of wood. a** | A scanning electron micrograph (SEM) of poplar wood depicting tracheids[124]. **b** | The hierarchical structure of an individual wood tracheid. **c** | An experimental stress–strain curve for spruce wood, showing large nonlinear strains and a progressive change in microfibril angle with deformation[133,142]. **d** | The deformation mechanism of a wood tracheid under axial tension, resembling that of a spring. The change in conformation of the spring-like tracheid involves shear deformations at the interface. The zoomed out schematic shows the key components of the interfibrillar interface and its Velcro-like behaviour. Panel **a** is reproduced with permission from REF. 124, Elsevier. Panel **c** is adapted with permission from REF. 142, © Carl Hanser Verlag, Muenchen.

Disrupting the finely tuned structures and mechanisms of these interfaces in bone can have a profound impact on overall performance. For example, suppressing key interface proteins, such as osteopontin, has immediate and dramatic consequences on overall toughness[83,94], and recent studies have shown that the decline in the mechanical properties of bone with age can be explained by the increase in covalent crosslinks at the nanointerfaces, which results in stiffness and brittleness[78]. These results clarify that bone must be understood as an integration of structural building blocks connected by interfaces.

The interfaces in wood

Wood is widely used in the construction industry because it is a relatively stiff and strong material; spruce wood has a modulus of 30 GPa and a strength of 300 MPa along the grain[119]. The work of fracture of wood is in the range of 15–30 kJ m^{-2}, which is comparable to that of metals such as aluminium and mild steel[120–122]. Wood has a cellular structure composed of parallel hollow tubes (known as cells or tracheids) that are about 20 inches in diameter[3,123] (FIG. 5a). Each tracheid is composed of several concentric secondary layers, the thickest being the S_2 layer (FIG. 5b), which accounts for approximately

© 2016 Macmillan Publishers Limited. All rights reserved

80–90% of the wood tracheid by weight and is its principal load-bearing element[5,124]. The S_2 layer is composed of laminates of cellulose microfibrils (about 45% by volume) that helically wind around the long axis of the tracheid and are embedded in a matrix of hemicelluloses (35% by volume; usually xylan and glucomannan) and lignin (20% by volume)[5,119] (FIG. 5b). The orientation of the microfibrils is characterized by the microfibril angle (MFA), which is defined as the angle between the fibrils and the axis of the tracheid. In the S_2 layer, the MFA can vary between 0° and 45° to the longitudinal axis[3,125]. Cellulose microfibrils are semicrystalline assemblies of cellulose molecules, with a diameter of approximately 10–25 nm. Cellulose is a high-molecular-weight polysaccharide with a covalent backbone, and, when part of the microfibril, cellulose molecules interact through the formation of covalent bonds and hydrogen bonds[126,127]. In the crystalline regions, the backbone of the molecules is aligned with the axis of the microfibrils, which makes microfibrils both very stiff (with an elastic modulus of 120–140 GPa) and very strong (with a tensile strength of 750–1,080 MPa)[119].

Hemicelluloses are very similar to cellulose, but they are more compliant because they lack the two hydrogen bonds flanking the glycosidic linkages in cellulose[128]. As a result, the elastic modulus of hydrated hemicellulose (about 20 MPa (REF. 129)) is three orders of magnitude lower than that of cellulose. Hemicelluloses can form hydrogen bonds with cellulose microfibrils, possibly by matching the patterns of hydrogen-bond-forming sites with those of cellulose and forming strong periodic patterns of hydrogen bonds[130]. Lignin is stiffer than hemicellulose under hydrated conditions but softer than cellulose. It has an elastic modulus of approximately 2 GPa under both dry and wet conditions[119,129,131]. In the S_2 layer, the hydrated mixture of hemicellulose and lignin has an elastic modulus of only about 0.75 GPa (evaluated using the rule of mixtures), which is about 170 times softer than the cellulose microfibrils. The S_2 layer is therefore composed of stiff and strong fibres that are bonded by much softer, nanometre-thick interfaces. Although it does not allow for dislocations, wood has a stress–strain behaviour similar to that of ductile metals (FIG. 5c). When loaded under tension along the direction of the tracheids, wood initially displays a linear elastic response, with a modulus strongly dependent on the MFA[121,132]. Wood then displays a yield point (at 10–20 MPa for compressive woods[133]) followed by large and irreversible deformation in excess of 20% strain and with pronounced strain hardening (FIG. 5c). The accumulation of damage in the hemicellulose, which was compensated by a reduction in the MFA and in stiffness, was proposed as a mechanism for large deformation[134]. However, these inelastic deformations are not accompanied by a decrease in stiffness, which implies that there is little or no accumulation of damage beyond the elastic limit[135].

In situ small-scale experiments and theoretical models have captured the deformation mechanisms of wood[128,133,136]. Recent studies include sophisticated computational models that incorporate interfaces and structures from the molecular scale to the mesoscale[137–140].

In situ X-ray tensile tests on wood and on isolated wood cells have revealed that the inelastic deformations can be attributed to micromechanisms within the wood cell walls[133,136]. More specifically, the helically wound cellulose microfibrils extend like springs and produce large strains, whereas the stiff microfibrils undergo little or no extension (FIG. 5d). In this process, the microfibrils align towards the direction of pulling, the MFA decreases (FIG. 5c) and the microfibrils slide on one another, which is resisted by the shearing of the interfaces. A Velcro-like recovery mechanism at the interface between cellulose fibrils has been proposed to explain the stiffness and strength recovery of wood after the release of stress[133]. When a critical shear stress at the interface is exceeded, the bonding — more specifically, the hydrogen bonds between hemicellulose chains and cellulose fibrils — breaks and re-forms to provide cohesive behaviour over a large sliding distance. When the stress is released, the bonds re-form so that the fibrils are locked into their deformed position, without the accumulation of damage or loss of stiffness[133]. It is possible that this Velcro-like behaviour is mediated by the hemicellulose and the lignin, which may entangle and disentangle in the shearing process[133,141] (FIG. 5d). However, this entanglement-based interaction may not be the only potential configuration at the interfaces between cellulose fibrils[142]. Other studies indicate that the entanglement cohesion of hemicellulose (specifically, xylans) is relatively weak and that a minimum length of approximately ten monomer residues of the hemicellulose segment is required for entanglement to produce substantial adhesion[141,143].

In a modified model for the Velcro-like mechanism, it has been proposed that the interfibrillar cohesion is mediated by hemicellulose chains that bridge adjacent cellulose macrofibrils[128] (FIG. 6a). The lateral binding between hemicellulose chains and cellulose fibrils requires that some of the hemicellulose chains form hydrogen bonds and align with the cellulose fibrils over some distance, forming discontinuous hemicellulose bridges across the interface[128,144]. When the interface is under stress, the hemicellulose loop may detach from one of the fibrils, which provides free length to the hemicellulose chain, releases some of the bridging strength and allows shear deformations between fibrils (FIG. 6b). When the stress is released, the hemicellulose loop can re-approach and re-attach to the cellulose fibrils through hydrogen bonding to maintain the overall stiffness. In this model for the hemicellulose chain segments between cellulose microfibrils, both entanglement and bridging cohesion could coexist[128] (FIG. 6a). These combined mechanisms were captured by mesoscale coarse-grain computational modelling[138]. The model demonstrated how entanglement and bridging govern the shearing of the interfaces, which occurs by the reconfiguration of the hemicellulose interface and by the 'stick–slip' of the hemicellulose, a phenomenon governed by the dynamic breaking and re-forming of hydrogen bonds at the interfaces between hemicellulose and cellulose, onto the cellulose microfibrils (FIG. 6c). This model also captured how large shear strains at

© 2016 Macmillan Publishers Limited. All rights reserved

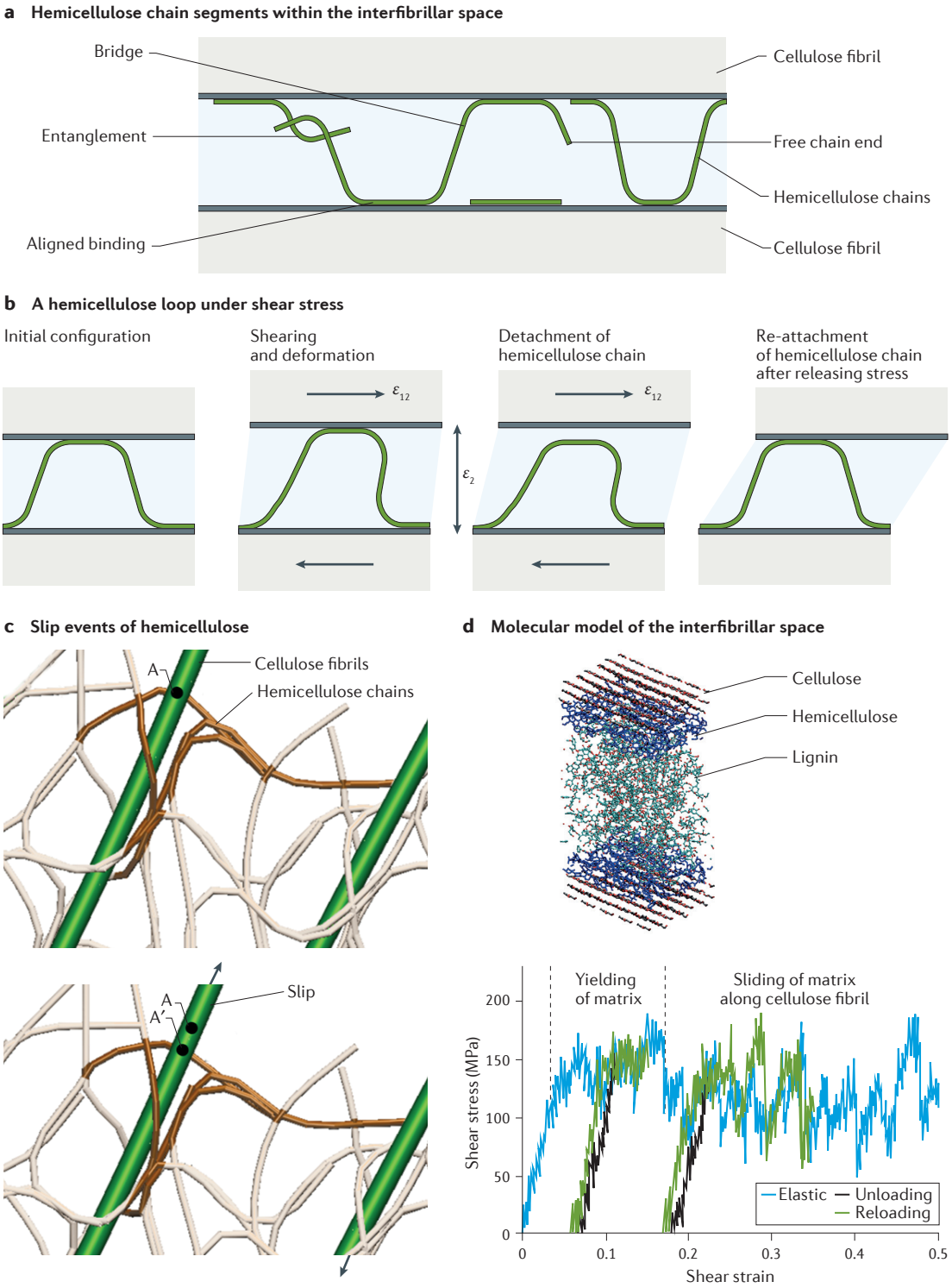

Figure 6 | **The structure and mechanics of the interfaces between cellulose fibrils. a** | Possible configurations of the hemicellulose chain segments within the interfibrillar space. **b** | A sequence showing the debonding of a hemicellulose loop from cellulose macrofibrils, and the re-approach and re-attachment after the releasing of shear stress as described in Altaner and Jarvis' model[128]. **c** | Slip events of hemicellulose captured in a coarse-grain model[138]. **d** | A more detailed atomistic model including cellulose crystals, hemicellulose and lignin. When this model is deformed under shear, an initial linear elastic region is followed by matrix yielding and then sliding of the matrix on the cellulose. Through these inelastic processes, the stiffness of the interface is preserved[137]. A, attachment point between hemicellulose and cellulose before slip; A′, attachment point between hemicellulose and cellulose after slip; ε_{12}, shear strain; ε_2, extensional across the interface. Panels **a** and **b** are adapted with permission from REF. 128, Elsevier. Panel **c** is adapted with permission from REF. 138, Royal Society of Chemistry. Panel **d** is adapted with permission from REF. 137, Elsevier.

© 2016 Macmillan Publishers Limited. All rights reserved

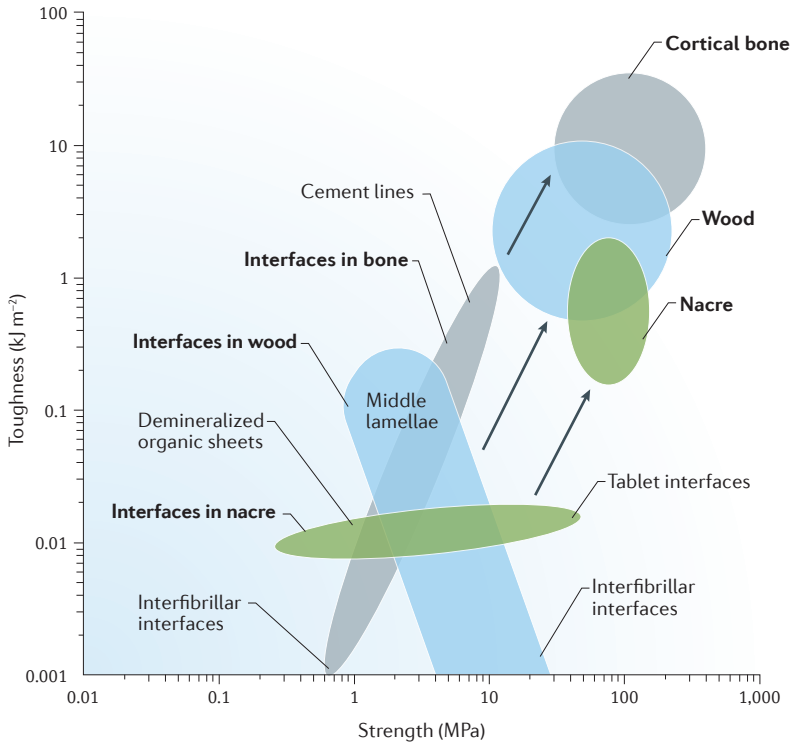

Figure 7 | **A material properties chart.** The toughness and strength for nacre[19,22,38], cortical bone[63,105], wood[149,150] and their interfaces[16,22,63,105,133,142,150].

the interfaces translate into large tensile strains at the macroscale through the cellulose MFAs. More recently, molecular models with atomistic resolution, and including the cellulose fibril, the hemicellulose and the lignin, revealed more details of these interfacial mechanisms[137] (FIG. 6d). These models uncovered an initial elastic response, followed by the yielding of the matrix. Finally, the matrix sled along the cellulose fibrils in a stick–slip manner. These molecular mechanisms provide cohesive stress during shear deformation over long sliding distances and without the loss of stiffness or strength, much like a dislocation motion in metals. Although the molecular mechanisms occurring at the interfibrillar interfaces have yet to be observed experimentally, the models reviewed here are based on the fundamental knowledge of the molecular interactions among hemicellulose, lignin and cellulose and therefore provide strong support for the Velcro-like mechanism.

Another important set of interfaces in wood consists of the middle lamellae, which bond the tracheids together[145] (FIG. 5a). This thin interface is composed of lignin (~50% by weight) and other compounds, such as pectic acids, arabinose and galactose[145–147], and it is weaker than the tracheid walls. The fracture of wood is a competition between the fracture of the tracheids and the fracture of the middle lamellae. In the splitting fracture direction, along the direction of the tracheids, wood is stressed in a tangential direction and the crack propagates in the longitudinal direction. In this configuration, cracks propagate along the middle lamellae, leaving the tracheids largely intact[148]. The splitting mode, in which wood is the weakest, provides estimates for the toughness[63,149] of the middle lamellae (0.1–0.3 kJ m^{-2}) and the tensile strength[63,150] in the order of 1–10 MPa, which is one to two orders of magnitude weaker than the toughness and strength of wood when it is fractured across the grains[63]. Experimental data and observations show that cracks propagating in wood strongly interact with the weak lamella interfaces[148,149]. From this point of view, wood can be described as a fibre-reinforced composite[149], in which the fibres are the individual tracheids, and the weaker middle lamellae govern toughening mechanisms, such as crack deflection and fibre pullout[149], in a similar way to osteons in cortical bone.

Summary and outlook

The examples discussed in this Review highlight the critical role of interfaces in the deformation and fracture of biological materials. A material properties chart (FIG. 7) of the strength and toughness of bone, nacre and wood, and their interfaces, illustrates that the strength and toughness of the interfaces are two to three orders of magnitude lower than the strength and toughness of the materials themselves. As a general rule, the interfaces must be sufficiently strong to maintain cohesion between the building blocks and to ensure the structural integrity of the material. However, the interface must be considerably weaker than the rest of the material to channel deformations and cracks, and for the intricate architectures to generate attractive mechanisms and properties. Models developed for synthetic layered ceramics can be useful as guidelines: for example, if an interface was designed to deflect cracks then its toughness should be less than one-quarter of the toughness of the surrounding material[151]. The case of ductile interfaces is more complex, but models now exist to guide the design of the interfacial strength[44,152].

Natural materials, such as mollusc shells, bone or wood, contain interfaces whose strength has been finely tuned through evolution to fulfil these conflicting requirements. The exact strength required is not a universal value, but it depends on the strength of the building blocks, the architecture of the building blocks, the loading mode of the material and, ultimately, its function within the larger organism. Another universal characteristic of interfaces in natural materials is their ability to maintain cohesion during openings or over sliding distances, which can be several times their thickness. These large deformations at the interface are critical for energy absorption and for producing large deformations at the macroscale, as well as powerful toughening mechanisms[37,153]. The interfaces of nacre, bone and wood illustrate three strategies to achieve this behaviour: first, organic materials show large deformations generated by molecular sacrificial bonds (as seen in nacre and in nanoscale bone); second, frictional forces provide resistance to interfacial sliding over unlimited sliding distances, as seen in nacre[19], at interfibrillar interfaces[95] and at the cement line[107] in bone; third, hydrogen bonds, which are inherently weak, can still provide appreciable cohesion in large coordinated numbers[154]. Hydrogen bonds can break and re-form dynamically, providing cohesion over long sliding distances (as seen in wood).

© 2016 Macmillan Publishers Limited. All rights reserved

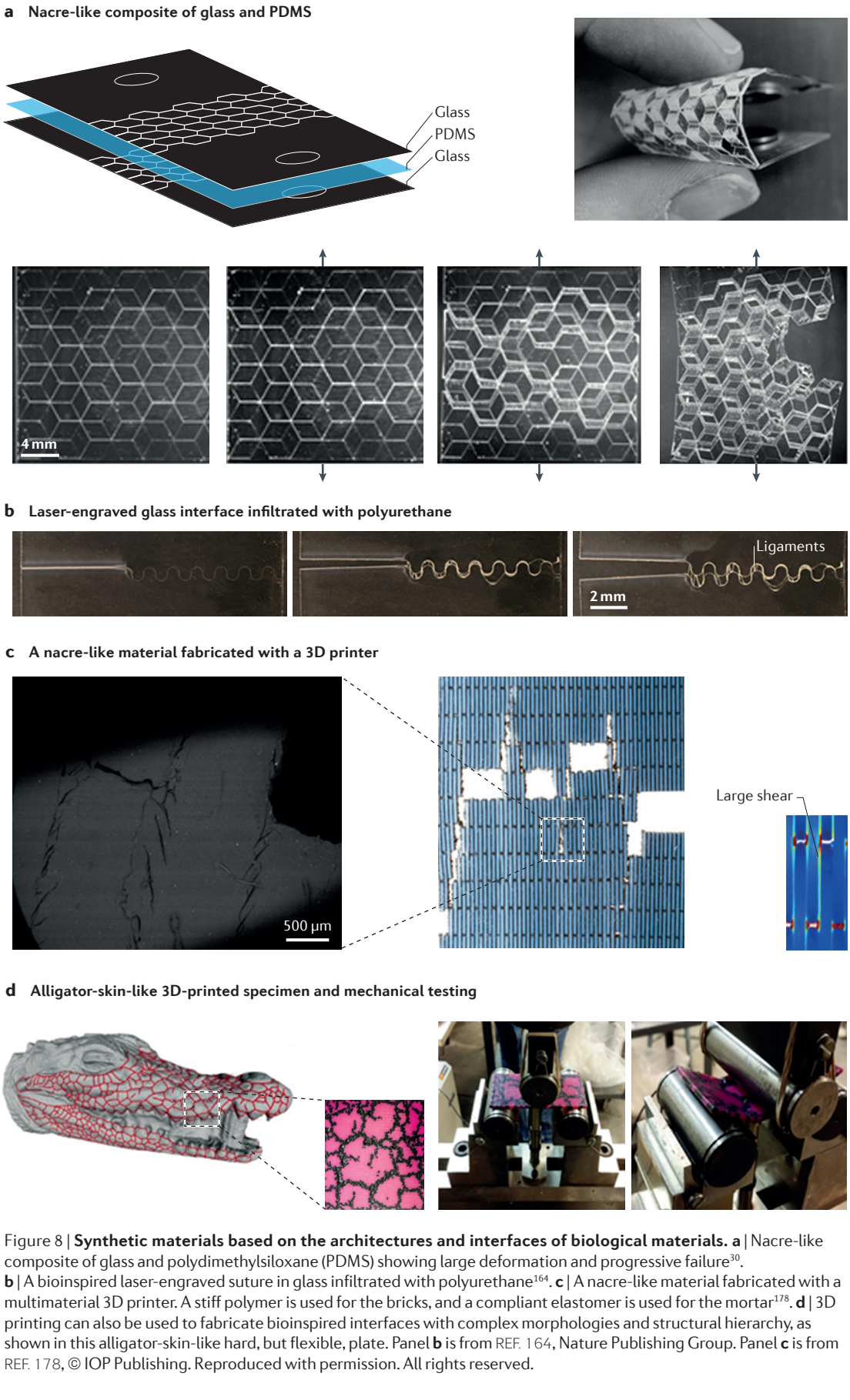

Figure 8 | **Synthetic materials based on the architectures and interfaces of biological materials. a** | Nacre-like composite of glass and polydimethylsiloxane (PDMS) showing large deformation and progressive failure[30]. **b** | A bioinspired laser-engraved suture in glass infiltrated with polyurethane[164]. **c** | A nacre-like material fabricated with a multimaterial 3D printer. A stiff polymer is used for the bricks, and a compliant elastomer is used for the mortar[178]. **d** | 3D printing can also be used to fabricate bioinspired interfaces with complex morphologies and structural hierarchy, as shown in this alligator-skin-like hard, but flexible, plate. Panel **b** is from REF. 164, Nature Publishing Group. Panel **c** is from REF. 178, © IOP Publishing. Reproduced with permission. All rights reserved.

© 2016 Macmillan Publishers Limited. All rights reserved

The composition and mechanics of the interfaces are finely tuned to interact with the architecture to produce desirable properties.

Nacre, bone and wood have different types of architectures, building blocks and interfaces, but the mechanical performance of the three materials relies on similar toughening mechanisms. The interfaces generate inelastic deformations at the nanoscale (as seen for bone and wood) or at the microscale (as seen for nacre). Large inelastic deformations redistribute stresses around defects and cracks[155], and reduce the sharpness of crack tips[98]. Inelastic deformations also dissipate mechanical energy that would otherwise be used to propagate cracks. This mechanism is prominent in nacre, and it serves as its main toughening mechanism, with a dissipative process zone in the order of millimetres in size forming around defects and cracks[37]. Other toughening mechanisms that are common to nacre, bone and wood are crack deflection and twisting, as well as crack bridging and fibre or tablet pullout. Interestingly, for bone and wood, ductility is generated at the nanoscale, although the most effective crack deflection and bridging mechanisms occur at the microscale.

The development of bioinspired composite materials that duplicate the mechanical performance of natural materials has been an active research area for the past two decades[2,6,9,20,29,156,157]. In particular, high-performance synthetic composites that mimic the architectures of natural materials have emerged. It is now clear that the performance of these composites relies on interfaces that mirror the attributes of natural interfaces. For example, polymers, such as acrylic foams[26], polymethylmethacrylate[158,159], polyvinyl alcohol[159,160] or chitosan[161], were used as interfaces between stiff ceramic layers or platelets to duplicate some of the attributes of the interfaces in nacre — namely, high adhesion, extensibility and energy absorption. To make the most of the ductility and energy absorption capabilities of the ductile polymers, the adhesion to the ceramic inclusions must be very strong, and surface functionalization with (3-aminopropyl)triethoxysilane is sometimes used to form covalent bonds between the polymer and the ceramic[161,162]. Partially crosslinked polymers or high-molecular-weight uncrosslinked polydimethylsiloxane have also achieved large strains via rheological flow[30] (FIG. 8a). In other cases, elastomers were used in combination with glass or rigid polymers in more complex bioinspired architectures[163,164] (FIG. 8b–d). Proteins with sacrificial bonds and the dynamic breaking and healing of hydrogen bonds can be duplicated using polymers with electric charges (polyelectrolytes)[162,165]. Bioinspired polymers with modular loops that display the same behaviour as proteins, such as lustrin A, were also successfully synthesized[27,166]. An interesting fabrication route is to use genetics to engineer biopolymeric interfaces with tunable properties[28]. Frictional interaction at the interfaces is also used in composites, most notably in fibre-reinforced composites but also in more recent bioinspired materials[164,167,168]. Recent methods, such as 3D laser engraving[164] (FIG. 8b) or multi-material 3D printing[163] (FIG. 8a,b), will enable the integration of complex architectures with tunable interface properties. Mechanisms at the interfaces and at the level of the architecture of the material operate in synergy to produce high properties at the macroscale. Capturing these synergies in synthetic materials presents challenges in terms of design and fabrication. Natural materials can inspire new strategies to design interfaces with attractive mechanical responses, which are essential for the design of advanced composite materials.

1. Sarikaya, M. & Aksay, I. A. *Biomimetic, Design and Processing of Materials* (Woodbury, 1995).
2. Mayer, G. Rigid biological systems as models for synthetic composites. *Science* **310**, 1144–1147 (2005).
3. Fratzl, P. & Weinkamer, R. Nature's hierarchical materials. *Prog. Mater. Sci.* **52**, 1263–1334 (2007).
4. Barthelat, F. Biomimetics for next generation materials. *Phil. Trans. R. Soc. A* **365**, 2907–2919 (2007).
5. Meyers, M. A., Chen, P.-Y., Lin, A. Y.-M. & Seki, Y. Biological materials: structure and mechanical properties. *Prog. Mater. Sci.* **53**, 1–206 (2008).
6. Espinosa, H. D., Rim, J. E., Barthelat, F. & Buehler, M. J. Merger of structure and material in nacre and bone — perspectives on *de novo* biomimetic materials. *Prog. Mater. Sci.* **54**, 1059–1100 (2009).
7. Nair, A. K. *et al.* in *Biomineralization Handbook: Characterization of Biomineral and Biomimetic Materials* (ed. DiMasi, E.) 337–349 (CRC Press, 2014).
8. Ritchie, R. O. The conflicts between strength and toughness. *Nat. Mater.* **10**, 817–822 (2011).
9. Naleway, S. E., Porter, M. M., McKittrick, J. & Meyers, M. A. Structural design elements in biological materials: application to bioinspiration. *Adv. Mater.* **27**, 5455–5476 (2015).
10. Barthelat, F. Architectured materials in engineering and biology: fabrication, structure, mechanics and performance. *Int. Mater. Rev.* **60**, 413–430 (2015).
11. Ackbarow, T. & Buehler, M. J. Hierarchical coexistence of universality and diversity controls robustness and multi-functionality in protein materials. *J. Comput. Theor. Nanosci.* **5**, 1193–1204 (2008).
12. Buehler, M. J. Tu(r)ning weakness to strength. *Nano Today* **5**, 379–383 (2010).
13. Cranford, S. & Buehler, M. J. *Biomateriomics* (Springer, 2012).
14. Dunlop, J. W. C., Weinkamer, R. & Fratzl, P. Artful interfaces within biological materials. *Mater. Today* **14**, 70–78 (2011).
15. Ritchie, R. O., Buehler, M. J. & Hansma, P. Plasticity and toughness in bone. *Phys. Today* **62**, 41–47 (2009).
16. Dastjerdi, A. K., Rabiei, R. & Barthelat, F. The weak interfaces within tough natural composites: experiments on three types of nacre. *J. Mech. Behav. Biomed. Mater.* **19**, 50–60 (2013).
17. Spivak, D. I., Giesa, T., Wood, E. & Buehler, M. J. Category theoretic analysis of hierarchical protein materials and social networks. *PLoS ONE* **6**, e23911 (2011).
18. Yahyazadehfar, M. & Arola, D. The role of organic proteins on the crack growth resistance of human enamel. *Acta Biomater.* **19**, 33–45 (2015).
19. Wang, R. Z., Suo, Z., Evans, A. G., Yao, N. & Aksay, I. A. Deformation mechanisms in nacre. *J. Mater. Res.* **16**, 2485–2493 (2001).
20. Barthelat, F. & Espinosa, H. D. An experimental investigation of deformation and fracture of nacre–mother of pearl. *Exp. Mech.* **47**, 311–324 (2007).
21. Currey, J. D. Mechanical properties of mother of pearl in tension. *Proc. R. Soc. Lond. B* **196**, 443–463 (1977).
22. Barthelat, F., Tang, H., Zavattieri, P. D., Li, C. M. & Espinosa, H. D. On the mechanics of mother of pearl: a key feature in the material hierarchical structure. *J. Mech. Phys. Solids* **55**, 306–337 (2007).
23. Weiner, S. & Wagner, H. D. The material bone: structure mechanical function relations. *Annu. Rev. Mater. Sci.* **28**, 271–298 (1998).
24. Rho, J. Y., Kuhn-Spearing, L. & Zioupos, P. Mechanical properties and the hierarchical structure of bone. *Med. Eng. Phys.* **20**, 92–102 (1998).
25. Giesa, T., Spivak, D. I. & Buehler, M. J. Category theory based solution for the building block replacement problem in materials design. *Adv. Eng. Mater.* **14**, 810–817 (2012).
26. Mayer, G. New classes of tough composite materials — lessons from natural rigid biological systems. *Mater. Sci. Eng. C* **26**, 1261–1268 (2006).
27. Kushner, A. M., Gabuchian, V., Johnson, E. G. & Guan, Z. Biomimetic design of reversibly unfolding cross-linker to enhance mechanical properties of 3D network polymers. *J. Am. Chem. Soc.* **129**, 14110–14111 (2007).
28. Laaksonen, P., Szilvay, G. R. & Linder, M. B. Genetic engineering in biomimetic composites. *Trends Biotechnol.* **30**, 191–197 (2012).
29. Studart, A. R. Towards high-performance bioinspired composites. *Adv. Mater.* **24**, 5024–5044 (2012).
30. Chintapalli, R. K., Breton, S., Dastjerdi, A. K. & Barthelat, F. Strain rate hardening: a hidden but critical mechanism for biological composites? *Acta Biomater.* **10**, 5064–5073 (2014).
31. Currey, J. D. & Taylor, J. D. The mechanical behavior of some molluscan hard tissues. *J. Zool.* **173**, 395–406 (1974).
32. Jackson, A. P., Vincent, J. F. V. & Turner, R. M. The mechanical design of nacre. *Proc. R. Soc. Lond. B* **234**, 415–440 (1988).
33. Colfen, H. & Antonietti, M. Mesocrystals: inorganic superstructures made by highly parallel crystallization and controlled alignment. *Angew. Chem. Int. Ed. Engl.* **44**, 5576–5591 (2005).

© 2016 Macmillan Publishers Limited. All rights reserved

34. Rousseau, M. *et al.* Multiscale structure of sheet nacre. *Biomaterials* **26**, 6254–6262 (2005).
35. Marin, F., Le Roy, N. & Marie, B. The formation and mineralization of mollusk shell. *Front. Biosci. (Schol. Ed.)* **4**, 1099–1125 (2012).
36. Li, X. D., Xu, Z. H. & Wang, R. Z. *In situ* observation of nanograin rotation and deformation in nacre. *Nano Lett.* **6**, 2301–2304 (2006).
37. Barthelat, F. & Rabiei, R. Toughness amplification in natural composites. *J. Mech. Phys. Solids* **59**, 829–840 (2011).
38. Rabiei, R., Bekah, S. & Barthelat, F. Failure mode transition in nacre and bone-like materials. *Acta Biomater.* **6**, 4081–4089 (2010).
39. Levi-Kalisman, Y., Falini, G., Addadi, L. & Weiner, S. Structure of the nacreous organic matrix of a bivalve mollusk shell examined in the hydrated state using cryo-TEM. *J. Struct. Biol.* **135**, 8–17 (2001).
40. Jackson, A. P. & Vincent, J. F. V. Application of surface analytical techniques to the study of fracture surfaces of mother of pearl. *J. Mater. Sci. Lett.* **5**, 975–978 (1986).
41. Menig, R., Meyers, M. H., Meyers, M. A. & Vecchio, K. S. Quasi-static and dynamic mechanical response of *Haliotis rufescens* (abalone) shells. *Acta Mater.* **48**, 2383–2398 (2000).
42. Lopez, M. I., Meza Martinez, P. E. & Meyers, M. A. Organic interlamellar layers, mesolayers and mineral nanobridges: contribution to strength in abalone (*Haliotis rufescence*) nacre. *Acta Biomater.* **10**, 2056–2064 (2014).
43. Shao, C. & Keten, S. Stiffness enhancement in nacre-inspired nanocomposites due to nanoconfinement. *Sci. Rep.* **5**, 16452 (2015).
44. Barthelat, F., Dastjerdi, A. K. & Rabiei, R. An improved failure criterion for biological and engineered staggered composites. *J. R. Soc. Interface* **10,** 20120849 (2013).
45. Nabavi, A., Capozzi, A., Goroshin, S., Frost, D. L. & Barthelat, F. A novel method for net-shape manufacturing of metal–metal sulfide cermets. *J. Mater. Sci.* **49**, 8095–8106 (2014).
46. Huang, Z. & Li, X. Nanoscale structural and mechanical characterization of heat treated nacre. *Mater. Sci. Eng. C* **29**, 1803–1807 (2009).
47. Marin, F., Luquet, G., Marie, B. & Medakovic, D. Molluscan shell proteins: primary structure, origin, and evolution. *Curr. Top. Dev. Biol.* **80**, 209–276 (2008).
48. Shen, X. Y., Belcher, A. M., Hansma, P. K., Stucky, G. D. & Morse, D. E. Molecular cloning and characterization of lustrin A, a matrix protein from shell and pearl nacre of *Haliotis rufescens*. *J. Biol. Chem.* **272**, 32472–32481 (1997).
49. Smith, B. L. *et al.* Molecular mechanistic origin of the toughness of natural adhesives, fibres and composites. *Nature* **399**, 761–763 (1999).
50. Vincent, J. F. V. & Wegst, U. G. K. Design and mechanical properties of insect cuticle. *Arthropod Struct. Dev.* **33**, 187–199 (2004).
51. Schaeffer, T. E. *et al.* Does abalone nacre form by heteroepitaxial nucleation or by growth through mineral bridges? *Chem. Mater.* **9**, 1731–1740 (1997).
52. Weiss, I. M. Jewels in the pearl. *ChemBioChem* **11**, 297–300 (2010).
53. Qi, H. J., Ortiz, C. & Boyce, M. C. Mechanics of biomacromolecular networks containing folded domains. *J. Eng. Mater. Technol.* **128**, 509–518 (2006).
54. Lopez, M. I. & Meyers, M. A. The organic interlamellar layer in abalone nacre: formation and mechanical response. *Mater. Sci. Eng. C* **58**, 7–13 (2016).
55. Weiss, I. M., Kaufmann, S., Heiland, B. & Tanaka, M. Covalent modification of chitin with silk-derivatives acts as an amphiphilic self-organizing template in nacre biomineralisation. *J. Struct. Biol.* **167**, 68–75 (2009).
56. Suetake, T. *et al.* Chitin-binding proteins in invertebrates and plants comprise a common chitin-binding structural motif. *J. Biol. Chem.* **275**, 17929–17932 (2000).
57. Suzuki, M. *et al.* An acidic matrix protein, Pif, is a key macromolecule for nacre formation. *Science* **325**, 1388–1390 (2009).
58. Laaksonen, P. *et al.* Genetic engineering of biomimetic nanocomposites: diblock proteins, graphene, and nanofibrillated cellulose. *Angew. Chem. Int. Ed. Engl.* **50**, 8688–8691 (2011).
59. Gent, A. N., Suh, J. B. & Kelly, S. G. Mechanics of rubber shear springs. *Int. J. Non-Linear Mechan.* **42**, 241–249 (2007).
60. Pascal, J., Darqueceretti, E., Felder, E. & Pouchelon, A. Rubber-like adhesive in simple shear — stress-analysis and fracture morphology of a single lap joint. *J. Adhes. Sci. Technol.* **8**, 553–573 (1994).
61. Song, F., Zhang, X. H. & Bai, Y. L. Microstructure and characteristics in the organic matrix layers of nacre. *J. Mater. Res.* **17**, 1567–1570 (2002).
62. Currey, J. D. *Bones: Structure and Mechanics* (Princeton Univ. Press, 2002).
63. Wegst, U. G. K. & Ashby, M. F. The mechanical efficiency of natural materials. *Philos. Mag.* **84**, 2167–2181 (2004).
64. Young, M. F. Bone matrix proteins: their function, regulation, and relationship to osteoporosis. *Osteoporosis Int.* **14**, S35–S42 (2003).
65. Hui, S. L., Slemenda, C. W. & Johnston, C. C. Age and bone mass as predictors of fracture in a prospective study. *J. Clin. Invest.* **81**, 1804–1809 (1988).
66. Burr, D. B. The contribution of the organic matrix to bone's material properties. *Bone* **31**, 8–11 (2002).
67. Reznikov, N., Shahar, R. & Weiner, S. Bone hierarchical structure in three dimensions. *Acta Biomater.* **10**, 3815–3826 (2014).
68. Buehler, M. J. Nature designs tough collagen: explaining the nanostructure of collagen fibrils. *Proc. Natl Acad. Sci. USA* **103**, 12285–12290 (2006).
69. Uzel, S. G. M. & Buehler, M. J. Molecular structure, mechanical behavior and failure mechanism of the C-terminal cross-link domain in type I collagen. *J. Mech. Behav. Biomed. Mater.* **4**, 153–161 (2011).
70. Shen, Z. L., Dodge, M. R., Kahn, H., Ballarini, R. & Eppell, S. J. Stress-strain experiments on individual collagen fibrils. *Biophys. J.* **95**, 3956–3963 (2008).
71. Hassenkam, T. *et al.* High-resolution AFM imaging of intact and fractured trabecular bone. *Bone* **35**, 4–10 (2004).
72. Buehler, M. J. Molecular nanomechanics of nascent bone: fibrillar toughening by mineralization. *Nanotechnology* **18,** 295102 (2007).
73. Knott, L. & Bailey, A. J. Collagen cross-links in mineralizing tissues: a review of their chemistry, function, and clinical relevance. *Bone* **22**, 181–187 (1998).
74. Launey, M. E., Buehler, M. J. & Ritchie, R. O. On the mechanistic origins of toughness in bone. *Annu. Rev. Mater. Res.* **40**, 25–53 (2010).
75. Ural, A. & Vashishth, D. Hierarchical perspective of bone toughness — from molecules to fracture. *Int. Mater. Rev.* **59**, 245–263 (2014).
76. Ritchie, R. O., Kinney, J. H., Kruzic, J. J. & Nalla, R. K. A fracture mechanics and mechanistic approach to the failure of cortical bone. *Fatigue Fract. Eng. Mater. Struct.* **28**, 345–371 (2005).
77. Thurner, P. J. & Katsamenis, O. L. The role of nanoscale toughening mechanisms in osteoporosis. *Curr. Osteoporosis Rep.* **12**, 351–356 (2014).
78. Zimmermann, E. A. *et al.* Age-related changes in the plasticity and toughness of human cortical bone at multiple length scales. *Proc. Natl Acad. Sci. USA* **108**, 14416–14421 (2011).
79. Taylor, D., Hazenberg, J. G. & Lee, T. C. Living with cracks: damage and repair in human bone. *Nat. Mater.* **6**, 263–268 (2007).
80. Gupta, H. S. *et al.* Fibrillar level fracture in bone beyond the yield point. *Int. J. Fracture* **139**, 425–436 (2006).
81. Fantner, G. E. *et al.* Sacrificial bonds and hidden length dissipate energy as mineralized fibrils separate during bone fracture. *Nat. Mater.* **4**, 612–616 (2005).
82. Gupta, H. S. *et al.* Nanoscale deformation mechanisms in bone. *Nano Lett.* **5**, 2108–2111 (2005).
83. Poundarik, A. A. *et al.* Dilatational band formation in bone. *Proc. Natl Acad. Sci. USA* **109**, 19178–19183 (2012).
84. Schwiedrzik, J. *et al. In situ* micropillar compression reveals superior strength and ductility but an absence of damage in lamellar bone. *Nat. Mater.* **13**, 740–747 (2014).
85. Nalla, R. K., Kinney, J. H. & Ritchie, R. O. Mechanistic fracture criteria for the failure of human cortical bone. *Nat. Mater.* **2**, 164–168 (2003).
86. Fantner, G. E. *et al.* Influence of the degradation of the organic matrix on the microscopic fracture behavior of trabecular bone. *Bone* **35**, 1013–1022 (2004).
87. Hang, F., Gupta, H. S. & Barber, A. H. Nanointerfacial strength between non-collagenous protein and collagen fibrils in antler bone. *J. R. Soc. Interface* **11,** 20130993 (2014).
88. Poundarik, A. A. & Vashishth, D. Multiscale imaging of bone microdamage. *Connect. Tissue Res.* **56**, 87–98 (2015).
89. Hansma, P. K. *et al.* Sacrificial bonds in the interfibrillar matrix of bone. *J. Musculoskelet. Neuronal Interact.* **5**, 313–315 (2005).
90. Gupta, H. S. *et al.* Evidence for an elementary process in bone plasticity with an activation enthalpy of 1 eV. *J. R. Soc. Interface* **4**, 277–282 (2007).
91. Seref-Ferlengez, Z., Basta-Pljakic, J., Kennedy, O. D., Philemon, C. J. & Schaffler, M. B. Structural and mechanical repair of diffuse damage in cortical bone *in vivo*. *J. Bone Miner. Res.* **29**, 2537–2544 (2014).
92. Thompson, J. B. *et al.* Bone indentation recovery time correlates with bond reforming time. *Nature* **414**, 773–776 (2001).
93. Fantner, G. E. *et al.* Nanoscale ion mediated networks in bone: osteopontin can repeatedly dissipate large amounts of energy. *Nano Lett.* **7**, 2491–2498 (2007).
94. Thurner, P. J. *et al.* Osteopontin deficiency increases bone fragility but preserves bone mass. *Bone* **46**, 1564–1573 (2010).
95. Tai, K., Ulm, F.-J. & Ortiz, C. Nanogranular origins of the strength of bone. *Nano Lett.* **6**, 2520–2525 (2006).
96. Bailey, A. J. Molecular mechanisms of ageing in connective tissues. *Mech. Ageing Dev.* **122**, 735–755 (2001).
97. Tang, S. Y., Zeenath, U. & Vashishth, D. Effects of non-enzymatic glycation on cancellous bone fragility. *Bone* **40**, 1144–1151 (2007).
98. Ker, R. F. Mechanics of tendon, from an engineering perspective. *Int. J. Fatigue* **29**, 1001–1009 (2007).
99. Puxkandl, R. *et al.* Viscoelastic properties of collagen: synchrotron radiation investigations and structural model. *Phil. Trans. R. Soc. Lond. B* **357**, 191–197 (2002).
100. Khayer Dastjerdi, A. & Barthelat, F. Teleost fish scales amongst the toughest collagenous materials. *J. Mech. Behav. Biomed. Mater.* **52**, 95–107 (2015).
101. Yang, W. *et al.* Protective role of *Arapaima gigas* fish scales: structure and mechanical behavior. *Acta Biomater.* **10**, 3599–3614 (2014).
102. Ascenzi, M.-G. & Roe, A. K. The osteon: the micromechanical unit of compact bone. *Front. Biosci. (Landmark Ed.)* **17**, 1551–1581 (2012).
103. Skedros, J. G., Holmes, J. L., Vajda, E. G. & Bloebaum, R. D. Cement lines of secondary osteons in human bone are not mineral-deficient: new data in a historical perspective. *Anat. Rec. A Discov. Mol. Cell Evol. Biol.* **286A**, 781–803 (2005).
104. Burr, D. B., Schaffler, M. B. & Frederickson, R. G. Composition of the cement line and its possible mechanical role as a local interface inhuman compact bone. *J. Biomech.* **21**, 939–945 (1988).
105. Koester, K. J., Ager, J. W., & Ritchie, R. O. The true toughness of human cortical bone measured with realistically short cracks. *Nat. Mater.* **7**, 672–677 (2008).
106. Ascenzi, A. & Bonucci, E. Shearing properties of single osteons. *Anat. Rec.* **172**, 499–510 (1972).
107. Bigley, R. F., Griffin, L. V., Christensen, L. & Vandenbosch, R. Osteon interfacial strength and histomorphometry of equine cortical bone. *J. Biomech.* **39**, 1629–1640 (2006).
108. Dong, X. N., Zhang, X. & Guo, X. E. Interfacial strength of cement lines in human cortical bone. *Mech. Chem. Biosyst.* **2**, 63–68 (2005).
109. O'Brien, F. J., Taylor, D. & Lee, T. C. Microcrack accumulation at different intervals during fatigue testing of compact bone. *J. Biomech.* **36**, 973–980 (2003).
110. Zioupos, P. & Currey, J. D. The extent of microcracking and the morphology of microcracks in damaged bone. *J. Mater. Sci.* **29**, 978–986 (1994).
111. Mellon, S. J. & Tanner, K. E. Bone and its adaptation to mechanical loading: a review. *Int. Mater. Rev.* **57**, 235–255 (2012).
112. Ager, J. W., Balooch, G. & Ritchie, R. O. Fracture, aging, and disease in bone. *J. Mater. Res.* **21**, 1878–1892 (2006).
113. Piekarsk, K. Fracture of bone. *J. Appl. Phys.* **41**, 215–223 (1970).
114. Hiller, L. P. *et al.* Osteon pullout in the equine third metacarpal bone: effects of *ex vivo* fatigue. *J. Orthopaed. Res.* **21**, 481–488 (2003).
115. Buehler, M. J. & Ackbarow, T. Fracture mechanics of protein materials. *Mater. Today* **10**, 46–58 (2007).
116. Zhang, Z., Zhang, Y.-W. & Gao, H. On optimal hierarchy of load-bearing biological materials. *Proc. R. Soc. B* **278**, 519–525 (2011).
117. Peterlik, H., Roschger, P., Klaushofer, K. & Fratzl, P. From brittle to ductile fracture of bone. *Nat. Mater.* **5**, 52–55 (2006).
118. Zioupos, P., Currey, J. D. & Sedman, A. J. An examination of the micromechanics of failure of bone and antler by acoustic emission tests and laser scanning confocal microscopy. *Med. Eng. Phys.* **16**, 203–212 (1994).

© 2016 Macmillan Publishers Limited. All rights reserved

119. Gibson, L. J. The hierarchical structure and mechanics of plant materials. *J. R. Soc. Interface* **9**, 2749–2766 (2012).
120. Jeronimidis, G. J. The fracture behavior of wood and the relations between toughness and morphology. *Proc. R. Soc. Lond. B* **208**, 447–460 (1980).
121. Gordon, J. E. & Jeronimidis, G. Composites with high work of fracture. *Phil. Trans. R. Soc. Lond. A* **294**, 545–550 (1980).
122. Lucas, P. W., Tan, H. T. W. & Cheng, P. Y. The toughness of secondary cell wall and woody tissue. *Phil. Trans. R. Soc. Lond. B* **352**, 341–352 (1997).
123. Fratzl, P. Cellulose and collagen: from fibres to tissues. *Curr. Opin. Colloid Interface Sci.* **8**, 145–155 (2003).
124. Pilate, G. *et al.* Lignification and tension wood. *C. R. Biol.* **327**, 889–901 (2004).
125. Lichtenegger, H., Reiterer, A., Stanzl-Tschegg, S. E. & Fratzl, P. Variation of cellulose microfibril angles in softwoods and hardwoods — a possible strategy of mechanical optimization. *J. Struct. Biol.* **128**, 257–269 (1999).
126. Jarvis, M. Cellulose stacks up. *Nature* **426**, 611–612 (2003).
127. Sinko, R., Qin, X. & Keten, S. Interfacial mechanics of cellulose nanocrystals. *MRS Bull.* **40**, 340–348 (2015).
128. Altaner, C. M. & Jarvis, M. C. Modelling polymer interactions of the 'molecular Velcro' type in wood under mechanical stress. *J. Theor. Biol.* **253**, 434–445 (2008).
129. Salmén, L. Micromechanical understanding of the cell-wall structure. *C. R. Biol.* **327**, 873–880 (2004).
130. Fratzl, P., Burgert, I. & Gupta, H. S. On the role of interface polymers for the mechanics of natural polymeric composites. *Phys. Chem. Chem. Phys.* **6**, 5575–5579 (2004).
131. Cousins, W. J. Elasticity of isolated lignin: Young's modulus by a continuous indentation method. *N. Z. J. For. Sci.* **7**, 107–112 (1977).
132. Cave, I. The anisotropic elasticity of the plant cell wall. *Wood Sci. Technol.* **2**, 268–278 (1968).
133. Keckes, J. *et al.* Cell-wall recovery after irreversible deformation of wood. *Nat. Mater.* **2**, 810–814 (2003).
134. Navi, P., Rastogi, P. K., Gresse, V. & Tolou, A. Micromechanics of wood subjected to axial tension. *Wood Sci. Technol.* **29**, 411–429 (1995).
135. Spatz, H., Köhler, L. & Niklas, K. J. Mechanical behaviour of plant tissues: composite materials or structures? *J. Exp. Biol.* **202**, 3269–3272 (1999).
136. Kohler, L. & Spatz, H. C. Micromechanics of plant tissues beyond the linear-elastic range. *Planta* **215**, 33–40 (2002).
137. Jin, K., Qin, Z. & Buehler, M. J. Molecular deformation mechanisms of the wood cell wall material. *J. Mech. Behav. Biomed. Mater.* **42**, 198–206 (2015).
138. Adler, D. C. & Buehler, M. J. Mesoscale mechanics of wood cell walls under axial strain. *Soft Matter* **9**, 7138–7144 (2013).
139. Liang, L., Perre, P., Frank, X. & Mazeau, K. A coarse-grain force-field for xylan and its interaction with cellulose. *Carbohydr. Polym.* **127**, 438–450 (2015).
140. Saavedra Flores, E. I., DiazDelao, F. A., Friswell, M. I. & Ajaj, R. M. Investigation on the extensibility of the wood cell-wall composite by an approach based on homogenisation and uncertainty analysis. *Compos. Struct.* **108**, 212–222 (2014).
141. Navi, P. & Heger, F. Combined densification and thermo–hydro-mechanical processing of wood. *MRS Bull.* **29**, 332–336 (2004).
142. Fratzl, P., Burgert, I. & Keckes, J. Mechanical model for the deformation of the wood cell wall. *Z. Metallkd.* **95**, 579–584 (2004).
143. Stiernstedt, J., Brumer, H., Zhou, Q., Teeri, T. T. & Rutland, M. W. Friction between cellulose surfaces and effect of xyloglucan adsorption. *Biomacromolecules* **7**, 2147–2153 (2006).
144. Åkerholm, M. & Salmén, L. Interactions between wood polymers studied by dynamic FT-IR spectroscopy. *Polymer* **42**, 963–969 (2001).
145. Wimmer, R. & Lucas, B. N. Comparing mechanical properties of secondary wall and cell corner middle lamella in spruce wood. *IAWA J.* **18**, 77–88 (1997).
146. Whiting, P. & Goring, D. A. I. Chemical characterization of tissue fractions from the middle lamella and secondary wall of black spruce tracheids. *Wood Sci. Technol.* **16**, 261–267 (1982).
147. Sorvari, J., Sjöström, E., Klemola, A. & Laine, J. E. Chemical characterization of wood constituents, especially lignin, in fractions separated from middle lamella and secondary wall of Norway spruce (*Picea abies*). *Wood Sci. Technol.* **20**, 35–51 (1986).
148. Thuvander, F. & Berglund, L. A. *In situ* observations of fracture mechanisms for radial cracks in wood. *J. Mater. Sci.* **35**, 6277–6283 (2000).
149. Ashby, M. F., Easterling, K. E., Harrysson, R. & Maiti, S. K. The fracture and toughness of woods. *Proc. R. Soc. Lond. A* **398**, 261–280 (1985).
150. United States Department of Agriculture. *Wood handbook: wood as an engineering material* (Forest Products Laboratory, 1974).
151. He, M. Y. & Hutchinson, J. W. Crack deflection at an interface between dissimilar elastic materials. *Int. J. Solids Struct.* **25**, 1053–1067 (1989).
152. Chan, K. S., He, M. Y. & Hutchinson, J. W. Cracking and stress redistribution in ceramic layered composites. *Mater. Sci. Eng. A* **167**, 57–64 (1993).
153. Gao, H. J. Application of fracture mechanics concepts to hierarchical biomechanics of bone and bone-like materials. *Int. J. Fracture* **138**, 101–137 (2006).
154. Keten, S., Xu, Z., Ihle, B. & Buehler, M. J. Nanoconfinement controls stiffness, strength and mechanical toughness of β-sheet crystals in silk. *Nat. Mater.* **9**, 359–367 (2010).
155. Evans, A. G. Design and life prediction issues for high-temperature engineering ceramics and their composites. *Acta Mater.* **45**, 23–40 (1997).
156. Sarikaya, M. An introduction to biomimetics: a structural viewpoint. *Microsc. Res. Tech.* **27**, 360–375 (1994).
157. Wegst, U. G. K., Bai, H., Saiz, E., Tomsia, A. P. & Ritchie, R. O. Bioinspired structural materials. *Nat. Mater.* **14**, 23–36 (2015).
158. Munch, E. *et al.* Tough, bio-inspired hybrid materials. *Science* **322**, 1516–1520 (2008).
159. Livanov, K. *et al.* Tough alumina/polymer layered composites with high ceramic content. *J. Am. Ceram. Soc.* **98**, 1285–1291 (2015).
160. Wang, J., Cheng, Q., Lin, L. & Jiang, L. Synergistic toughening of bioinspired poly(vinyl alcohol)–clay–nanofibrillar cellulose artificial nacre. *ACS Nano* **8**, 2739–2745 (2014).
161. Bonderer, L. J., Studart, A. R. & Gauckler, L. J. Bioinspired design and assembly of platelet reinforced polymer films. *Science* **319**, 1069–1073 (2008).
162. Cavelier, S., Barrett, C. J. & Barthelat, F. The mechanical performance of a biomimetic nanointerface made of multilayered polyelectrolytes. *Eur. J. Inorg. Chem.* **2012**, 5380–5389 (2012).
163. Dimas, L. S., Bratzel, G. H., Eylon, I. & Buehler, M. J. Tough composites inspired by mineralized natural materials: computation, 3D printing, and testing. *Adv. Funct. Mater.* **23**, 4629–4638 (2013).
164. Mirkhalaf, M., Dastjerdi, A. K. & Barthelat, F. Overcoming the brittleness of glass through bio-inspiration and micro-architecture. *Nat. Commun.* **5**, 3166 (2014).
165. Tang, Z. Y., Kotov, N. A., Magonov, S. & Ozturk, B. Nanostructured artificial nacre. *Nat. Mater.* **2**, 413–418 (2003).
166. Guan, Z. Supramolecular design in biopolymers and biomimetic polymers for properties. *Polym. Int.* **56**, 467–473 (2007).
167. Barthelat, F. & Zhu, D. J. A novel biomimetic material duplicating the structure and mechanics of natural nacre. *J. Mater. Res.* **26**, 1203–1215 (2011).
168. Bouville, F. *et al.* Strong, tough and stiff bioinspired ceramics from brittle constituents. *Nat. Mater.* **13**, 508–514 (2014).
169. Ashby, M. *Materials Selection in Mechanical Design* 4th edn (Butterworth–Heinemann, 2010).
170. Evans, A. G. Perspective on the development of high-toughness ceramics. *J. Am. Ceram. Soc.* **73**, 187–206 (1990).
171. Clegg, W. J., Kendall, K., Alford, N. M., Button, T. W. & Birchall, J. D. A simple way to make tough ceramics. *Nature* **347**, 455–457 (1990).
172. Cook, J., Gordon, J. E., Evans, C. C. & Marsh, D. M. A mechanism for the control of crack propagation in all-brittle systems. *Proc. R. Soc. Lond. A* **282**, 508–520 (1964).
173. Kim, J.-K. & Mai, Y.-W. *Engineered Interfaces in Fier Reinforced Composites* (Elsevier Sciences, 1998).
174. Yu, H. N., Longana, M. L., Jalalvand, M., Wisnom, M. R. & Potter, K. D. Pseudo-ductility in intermingled carbon/glass hybrid composites with highly aligned discontinuous fibres. *Composites, Part A* **73**, 35–44 (2015).
175. Baldan, A. Adhesively-bonded joints and repairs in metallic alloys, polymers and composite materials: adhesives, adhesion theories and surface pretreatment. *J. Mater. Sci.* **39**, 1–49 (2004).
176. Gent, A. N. & Lindley, P. B. Internal rupture of bonded rubber cylinders in tension. *Proc. R. Soc. Lond. A* **249**, 195–205 (1959).
177. Mooney, M. Stress–strain curves of rubbers in simple shear. *J. Appl. Phys.* **35**, 23–26 (1964).
178. Qin, Z., Dimas, L., Adler, D., Bratzel, G. & Buehler, M. J. Biological materials by design. *J. Phys. Condens. Matter* **26**, 073101 (2014).
179. Mirzaeifar, R., Dimas, L. S., Qin, Z. & Buehler, M. J. Defect-tolerant bioinspired hierarchical composites: simulation and experiment. *ACS Biomater. Sci. Eng.* **1**, 295–304 (2015).
180. Dimas, L. S. & Buehler, M. J. Modeling and additive manufacturing of bio-inspired composites with tunable fracture mechanical properties. *Soft Matter* **10**, 4436–4442 (2014).

Acknowledgements
Z.Y. was partially supported by a McGill Engineering Doctoral Award from the Faculty of Engineering at McGill University.

Competing interests statement
The authors declare no competing interests.

© 2016 Macmillan Publishers Limited. All rights reserved